

1 **The initiation of the wound healing program is regulated by the convergence of**
2 **mechanical and epigenetic cues**

3

4

5 Tanay Bhatt^{1,2}, Rakesh Dey¹, Akshay M. Hegde¹, Alhad Ashok Ketkar³, Ajai J.

6 Pulianmackal^{1,*}, Ashim P. Deb¹, Shravanti Rampalli^{3,#}, Colin Jamora^{1,δ}

7

8 1. IFOM-inStem Joint Research Laboratory, Center for Inflammation and Tissue
9 Homeostasis, Institute for Stem Cell Science and Regenerative Medicine,
10 Bangalore

11 2. National Centre for Biological Sciences, Bangalore

12 3. Center for Inflammation and Tissue Homeostasis, Institute for Stem Cell Science
13 and Regenerative Medicine, Bangalore

14

15 * Current address = Department of Molecular, Cellular and Developmental Biology,
16 University of Michigan

17

18 # Current address = CSIR - Institute for Genomics and Integrative Biology, New Delhi

19

20 δ Corresponding author: Colin Jamora, colinj@instem.res.in

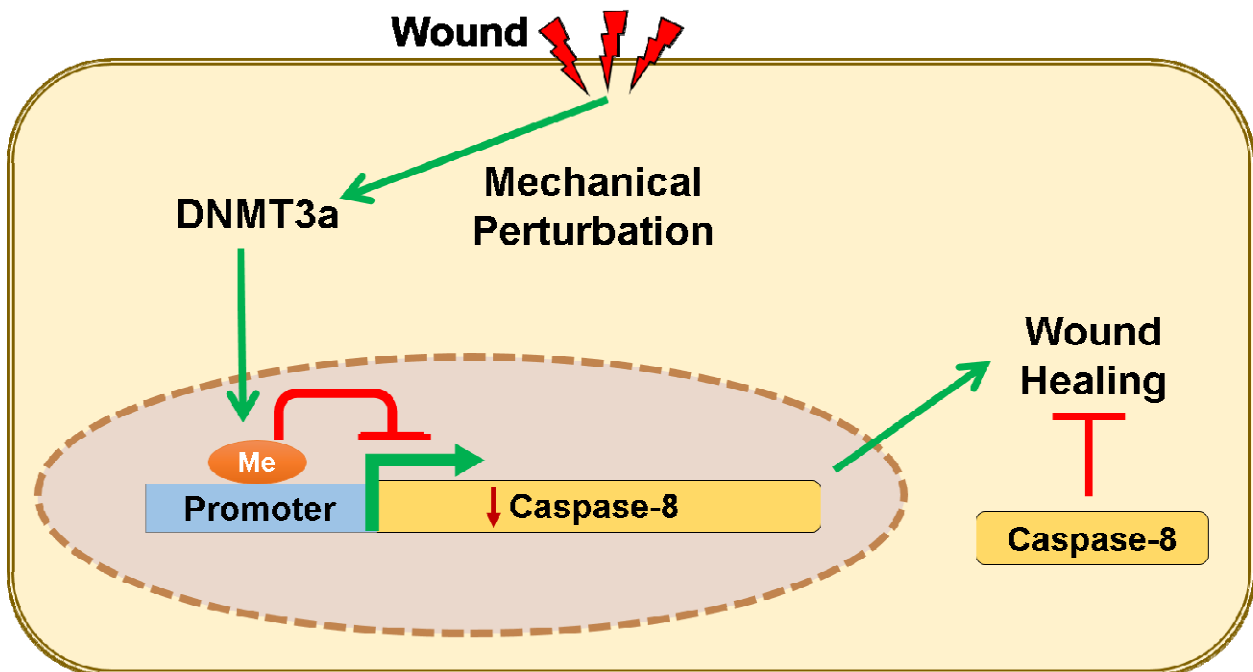
21 **ABSTRACT**

22

23 Wound healing in the skin is a complex physiological process that is a product of a cell
24 state transition from homeostasis to repair. Mechanical cues are increasingly being
25 recognized as important regulators of cellular reprogramming, but the mechanism by
26 which it is translated to changes in gene expression and ultimately cellular behavior
27 remains largely a mystery. To probe the molecular underpinnings of this phenomenon
28 further, we used the downregulation of caspase-8 as a biomarker of a cell entering the
29 wound-healing program. We found that the wound-induced release of tension within the
30 epidermis leads to the alteration of gene expression via the nuclear translocation of the
31 DNA methyltransferase 3A (DNMT3a). This enzyme then methylates promoters of
32 genes that are known to be downregulated in response to wound stimuli as well as
33 potentially novel players in the repair program. Overall, these findings illuminate the
34 convergence of mechanical and epigenetic signaling modules that are important
35 regulators of the transcriptome landscape required to initiate the tissue repair process in
36 the differentiated layers of the epidermis.

37

38 **Graphical Abstract:**



39 Introduction

40 The wound healing program in an epithelial tissue is fundamentally a product of cell
41 state transitions from homeostasis to a repair program. In particular, cutaneous wound
42 healing in the adult is an intricately regulated system wherein keratinocytes and many
43 other cell lineages exhibit their plasticity as they undergo reprogramming, to carry out
44 otherwise dormant functions, to rebuild the damaged skin. Many of the phenomena that
45 occur in the repair process in adult skin are, in fact, reminiscent of cellular events that
46 operate during fetal development (1). At the other extreme, inappropriate activation of
47 these repair processes can manifest as tissue pathology, which forms the foundation of
48 the perception of diseases with a “wound signature” (2). The question that arises is
49 how the whole scale changes in gene expression are accomplished in order to facilitate
50 this cellular reprogramming.

51 Recently, epigenetic regulators have emerged as a vital component capable of
52 transiently rewiring the cell’s transcriptional program to mediate the continual
53 regeneration of the mouse epidermis (3, 4). This mode of gene regulation operates at
54 multiple levels ranging from histone and DNA modifications, chromatin remodeling, and
55 activity of various subtypes of RNA species such as non-coding RNAs and micro-RNAs
56 (miRNAs) (5, 6). These epigenetic mechanisms can thus have a profound impact on
57 the transcriptional landscape of the cell, and can easily be envisioned to participate in
58 the transient activation or repression of the ~1000 genes that are required for wound
59 closure (7). However, relative to the appreciation of epigenetics in epidermal
60 homeostasis, the understanding of its role in wound healing remains an area ripe for
61 further exploration. Circumstantial evidence in support of a role for epigenetics in tissue
62 repair comes from reports of their dynamic expression following injury to the skin. For
63 instance, Ezh2, Suz12, and Eed, which are components of the Polycomb Repressive
64 Complex 2 (PRC2), are downregulated, whereas the histone methylases JMJD3 and
65 Utx are upregulated upon tissue damage and all return to homeostatic levels upon the
66 completion of wound closure (8). While the description of various epigenetic players in
67 epidermal homeostasis and wound-healing are reported, the identity and function of
68 their upstream regulators are, to a large extent, absent in the literature.

69 An intriguing candidate for an upstream regulator in a highly tensile tissue such as the
70 epidermis, are mechanical cues. The epidermis is a stratified epithelium comprised of a
71 basal layer of proliferation competent keratinocytes and suprabasal layers of
72 differentiated cells glued together via intercellular adhesion complexes that partly
73 endows the tissue with its barrier function. In different cell types, changes in
74 mechanical tension have been documented to induce the nuclear translocation of
75 important transcription factors - a notable example of which is YAP/TAZ that has
76 proliferation stimulating gene targets (9). Many studies, including those on epidermal
77 homeostasis and wound healing, have primarily focused on the changes in gene
78 expression in proliferating cells (10, 11). On the other hand, differentiated cells, such
79 as the suprabasal keratinocytes near the surface of the epidermis, have largely been
80 relegated to bystander status. In spite of this, a few reports suggest that these
81 neglected pools of differentiated cells are not inert in the cellular crosstalk that mediates
82 the early responses of the tissue to injury. In particular, the uppermost layer of
83 differentiated keratinocytes in the epidermis express caspase-8 that has a non-
84 canonical role in regulating the wound-healing program. We previously demonstrated
85 that the downregulation of caspase-8 is a natural phenomenon upon application of an
86 excisional wound to the mouse skin (12). This downregulation is particularly relevant as
87 genetically ablating caspase-8 in the epidermis is sufficient to induce a wound healing
88 response even in the absence of any damage to the organ. In addition, the
89 downregulation of caspase-8 in the upper, differentiated, layer of the epidermis
90 mediates signaling networks to incite epithelial stem cell proliferation in the epidermis
91 (12) and the hair follicle (13, 14) to fuel wound closure. We have thus used the
92 downregulation of caspase-8 as a cellular biomarker to identify the higher order
93 regulatory machinery that reprograms the cell to enter the wound healing process in
94 differentiated keratinocytes, which are emerging as an important participant in the tissue
95 repair program.

96

97 **Wound induce downregulation of caspase-8 RNA correlates with the degree of**
98 **promoter methylation**

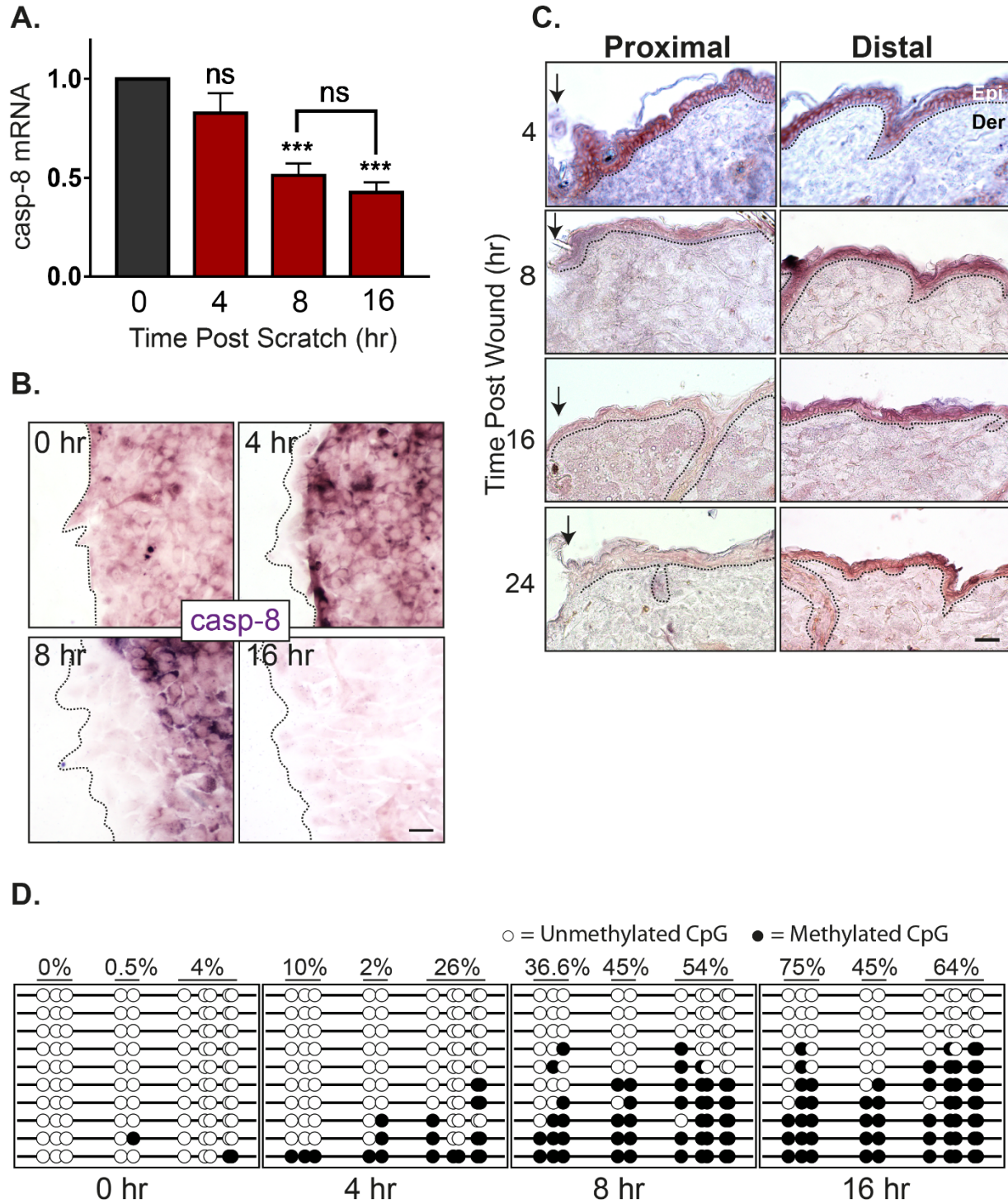
99

100 Previously, we have established the importance of the downregulation of caspase-8
101 RNA in both physiological (wound healing (12)) as well as pathological (atopic
102 dermatitis (15) and psoriasis (16)) scenarios. The mechanisms responsible for this
103 downregulation, however, remains unknown. Uncovering the regulatory machinery of
104 caspase-8 RNA also holds the promise of understanding the process by which cells
105 transition from a state of homeostasis to repair. Moreover, it can provide potential new
106 therapeutic targets for common inflammatory skin diseases where this regulation is
107 perturbed.

108

109 RNA downregulation can be achieved either via blocking the synthesis and/or active
110 degradation. In order to distinguish between these two possibilities, we determined the
111 half-life of caspase-8 in homeostasis compared to wound conditions. In differentiated
112 primary epidermal keratinocytes, we observed that the half-life of caspase-8 mRNA
113 under homeostatic conditions in vitro is approximately 2 hours (Figure S1A). In an in
114 vitro scratch wound assay with multiple scratches, the level of caspase-8 RNA is
115 significantly reduced by 8 hours (Figure 1A). Since the reduction of caspase-8 is faster
116 under homeostatic conditions compared to the wound healing context, merely blocking
117 RNA synthesis can achieve the reduction of caspase-8 mRNA and initiate the
118 downstream wound healing response. Interestingly, the reduction caspase-8 RNA is
119 localized in cells near the front of the scratch wound in vitro (Figure 1B, Figure S1B). In
120 situ hybridization of caspase-8 RNA demonstrates that the downregulation can clearly
121 be visualized in the cells immediately adjacent to the leading edge of a single scratch
122 wound as early as 4 hours post wounding. By 8 hours post-wounding, the caspase-8
123 RNA is downregulated in about 3-4 cell layers from the wound front. These findings
124 are consistent with our observation in excisional wounds on the back skin of mice where
125 the decrease of caspase-8 RNA is visible as early as 4 hours in the wound proximal
126 region (Figure 1C and Figure S1C). Together these results suggest that simply
127 blocking transcription post injury is sufficient to downregulate caspase-8. We

128 hypothesized that the block in caspase-8 RNA synthesis is achieved through promoter
129 methylation, which is consistent with previous reports documenting the same
130 phenomenon in a variety of cancer cells through the hypermethylation of regulatory
131 DNA sequence(17, 18). To understand whether this process in cancer cells is an
132 aberration of the physiological healing program, we have assessed the methylation
133 status of important regulatory sequences in the caspase-8 promoter, namely the CpG
134 loci and SP1 binding sites (Figure S1D) (19). Analysis of methylation of SP1 sites and
135 other CpG loci reveals a time-dependent increase of promoter methylation in a sheet of
136 differentiated epidermal keratinocytes subjected to multiple scratch wounds (Figure 1D).
137 This progressive increase in the methylation of the caspase-8 promoter correlates well
138 with the kinetics of the decrease in caspase-8 RNA (Figure 1A-C). This suggest DNA
139 methylation may play a critical role in regulating the wound-healing response.



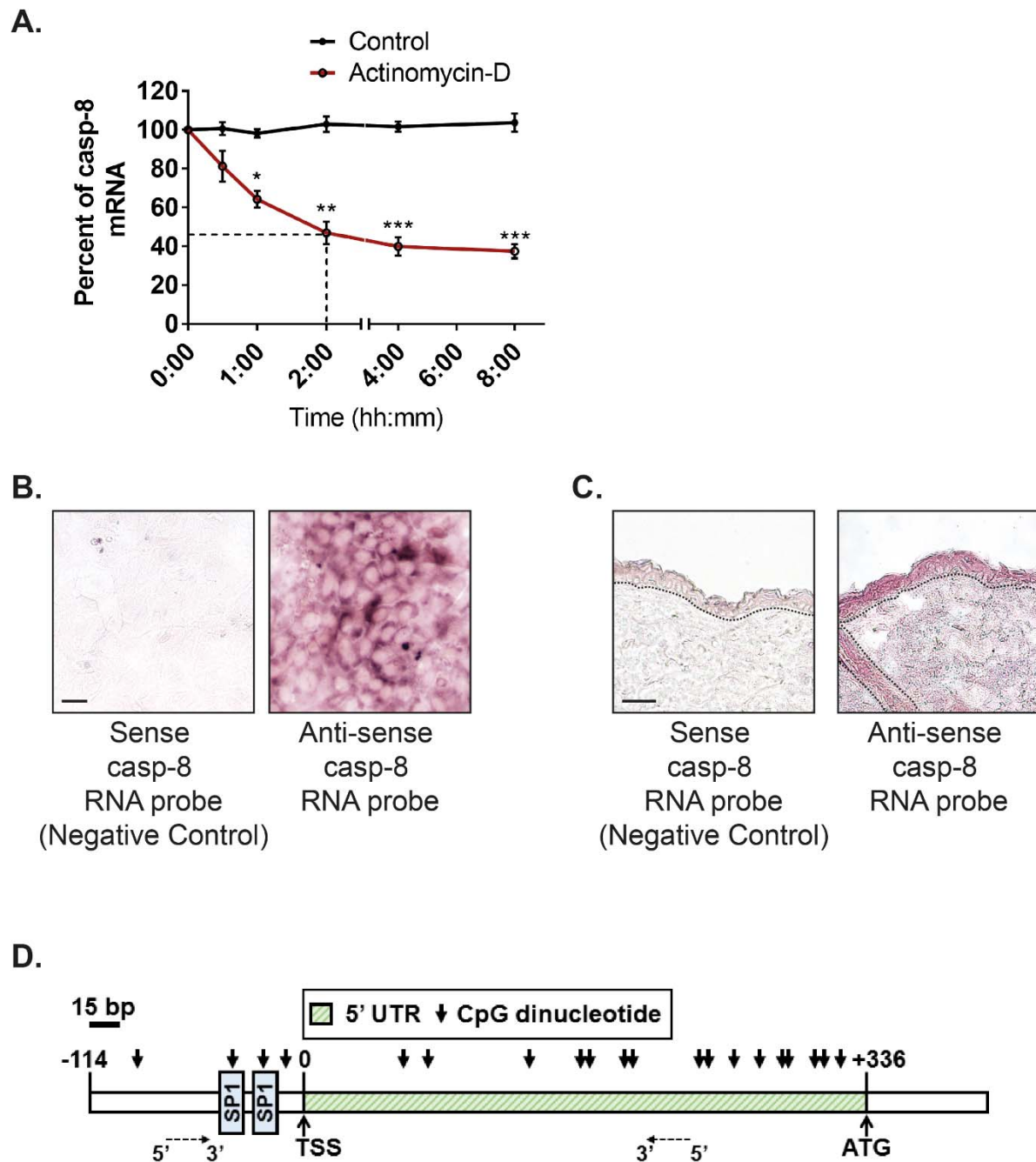
140

141 **Figure 1: Kinetics of caspase-8 promoter methylation and expression: A,** Levels of

142 caspase-8 mRNA at different time-points post scratch wound (fold change) (n=4) **B,** In-

143 vitro ISH of caspase-8 mRNA showing its levels at scratch-margins over time [scale =

144 10 μm] **C**, In-vivo ISH of caspase-8 mRNA showing its levels at wound proximal and
145 distal regions over time (dotted line represents basement membrane, Epi = Epidermis,
146 Der = Dermis) [scale = 20 μm] **D**, Bisulphite sequencing of caspase-8 promoter proximal
147 region (265bp) shows methylation status of 10 individual CpG sites (columns) from 10
148 cloned PCR products (rows) at various time-points post scratch wound. Percentage
149 value denotes the percent methylation for each group of CpG sites over time (Refer
150 Figure S1D for the sequenced region and primer sites). (Data are shown as
151 mean \pm SEM, P values were calculated using one-way ANOVA with Dunnett's test
152 and two-tailed t test (A), *** $P \leq 0.001$, ns = $P > 0.05$)



153 **Figure S1: caspase-8 RNA half-life and CpG positions on its promoter proximal**
 154 **region**

155 **A**, Quantification of caspase-8 mRNA to check its half-life post transcriptional block
 156 (using Actinomycin-D) **B**, In-situ hybridization with anti-sense and sense probe of

157 caspase-8 RNA (in-vitro) [scale = 10 μ m] **C**, In-situ hybridization with anti-sense and
158 sense probe of caspase-8 RNA (in-vivo) [scale = 20 μ m] **D**, Model showing positions of
159 CpG dinucleotide and SP1 binding sites in caspase-8 promoter proximal region (Data
160 are shown as mean \pm SEM, P values were calculated using one-way ANOVA with
161 Dunnett's test (A), * P \leq 0.05, ** P \leq 0.01, *** P \leq 0.001, ns = P > 0.05)

162 **Wound stimuli induce the nuclear localization of the DNA methyltransferase**
163 **DNMT3a**

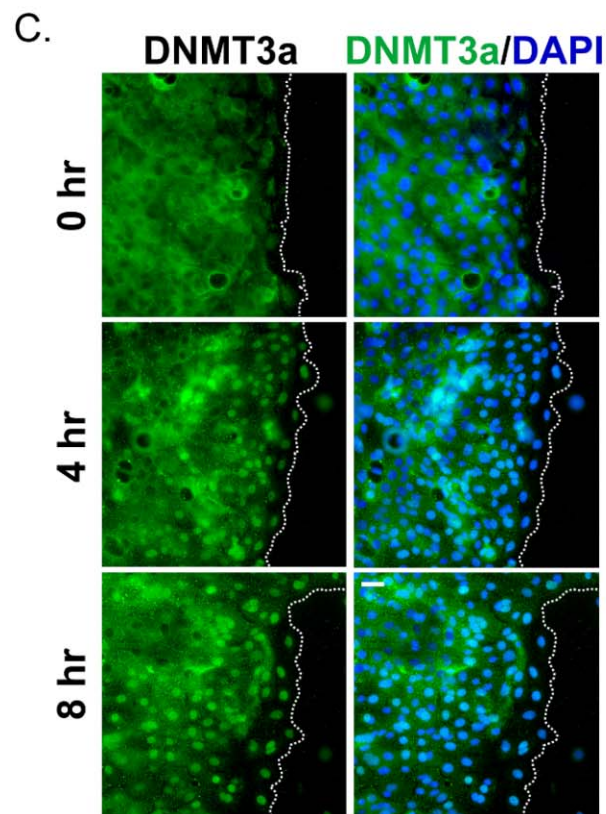
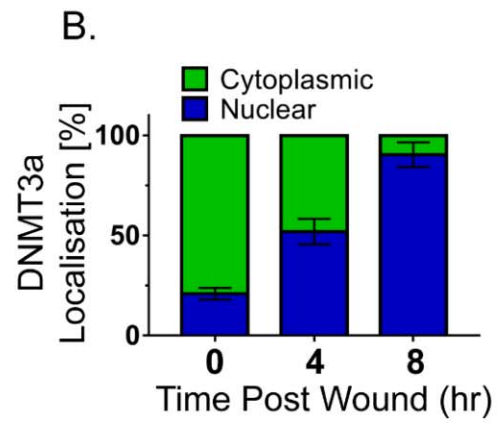
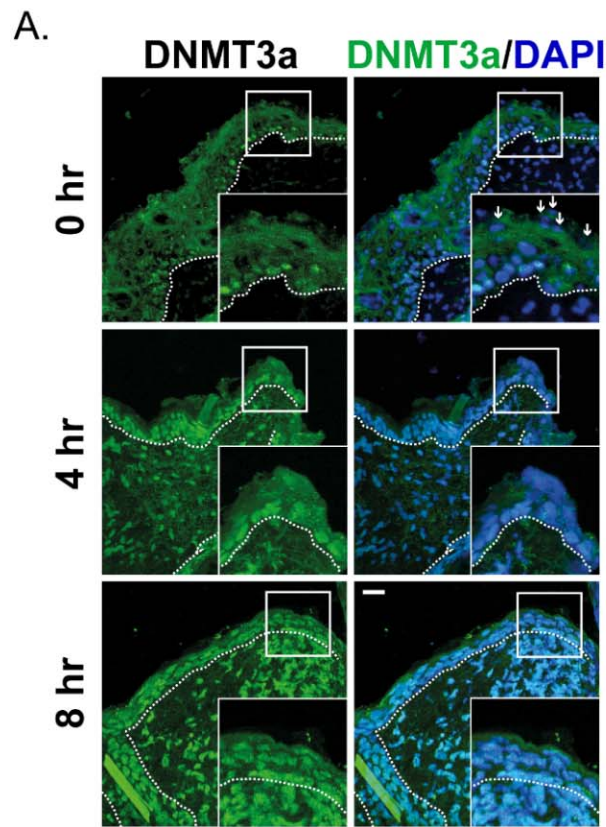
164

165 We thus investigated the mechanism responsible for DNA methylation of the caspase-8
166 promoter in response to injury. The bisulfite sequencing data reveals that the
167 methylation of the caspase-8 promoter is a de novo event in response to wounding. We
168 therefore examined the status of the two known de novo DNA methyltransferases
169 (DNMTs), namely DNMT3a and DNMT3b, in response to injury. Interestingly, de-novo
170 DNMTs (DNMT3a and 3b) have also been shown to be important in regulating
171 epidermal stem cell homeostasis (4). To investigate whether these enzymes likewise
172 play a role in tissue repair, we examined their expression in the wounded epidermis.
173 Consistent with a previous report, under homeostatic conditions, we found that DNMT3a
174 mainly resides in the nucleus of the basal/proliferating (K5 positive) cells and is absent
175 or cytoplasmic in the suprabasal/differentiated (K5 negative) keratinocytes (Figure S2A-
176 B) (20). This localization was also recapitulated in vitro wherein we observed the
177 cytosolic localization of DNMT3a in differentiated primary epidermal keratinocytes
178 (Figure S2C). Interestingly, in vivo we observed that DNMT3a undergoes cytoplasmic to
179 nuclear translocation in cells adjacent to the wound (Figure 2A). Quantification of the
180 nuclear vs. cytoplasmic localization of DNMT3a revealed a time dependent
181 accumulation of the enzyme in the nucleus post wounding (Figure 2B). This
182 phenomenon was more apparent in an in vitro scratch assay, where keratinocytes
183 adjacent to the scratch exhibited nuclear localization of DNMT3a (Figure 2C). The
184 second known de-novo DNMT, DNMT3b, also showed cytoplasmic localization in
185 differentiated keratinocytes (Figure S2D). However, it did not translocate to the nuclei of
186 scratch proximal keratinocytes (Figure S2E).

187

188 Thus, we focused on understanding the mechanistic details of DNMT3a's role in
189 regulating wound-healing program. The increase in DNMT3a nuclear localization was
190 time dependent, affecting wound proximal keratinocytes first and then moves towards
191 distal cells. At the completion of the wound-healing program we observe that DNMT3a
192 localization is again prominent within the cytoplasm of differentiated (K5 negative)

193 keratinocytes, while nuclear localization is restricted to cells in the basal layer of the
194 epidermis (Figure S2F). In conclusion, we observe that the DNMT3a shows significant
195 nuclear localisation in the wound-proximal (leading edge) cells within 4 hours of the
196 injury and the localisation pattern further penetrates in the distal regions as time passes
197 (Figure 2C). The nuclear localization kinetics also correlates with the pattern of
198 caspase-8 downregulation as well as promoter methylation (Figure 1B-D).

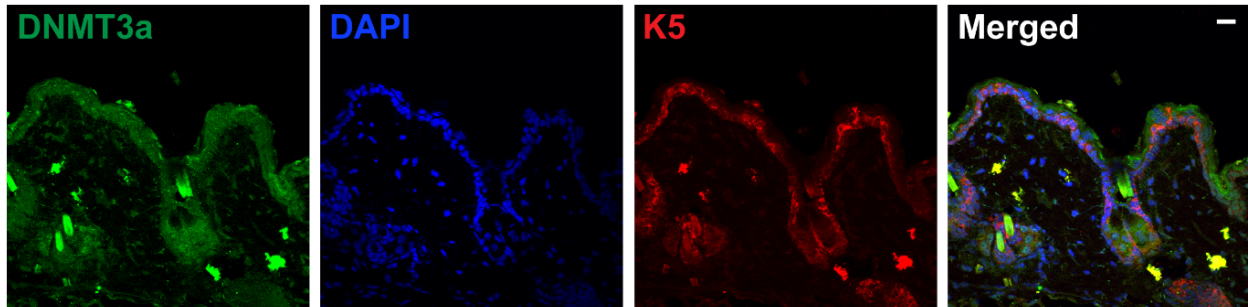


200 **Figure 2: A**, DNMT3a and DAPI staining of wound proximal (<0.5 mm) skin sections at
201 different time interval (small white arrows showing nuclei of suprabasal keratinocytes,
202 negative for DNMT3a staining. **B**, Quantification and kinetics of DNMT3a localization
203 (nuclear v/s cytoplasmic) from wound proximal ($\leq 100\mu\text{m}$) skin sections. (it represents
204 quantification of differentiating keratinocytes from the skin sections of three separate
205 biological replicates) **C**, DNMT3a and DAPI staining of scratch wounded in vitro
206 differentiated keratinocyte layer [scale = 20 μm]

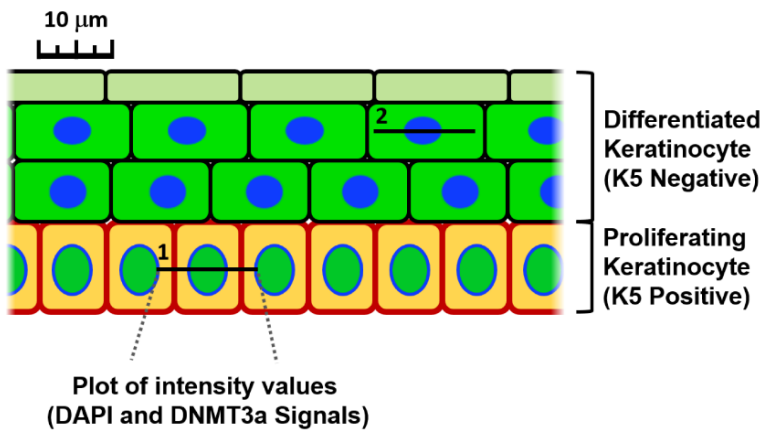
207

208

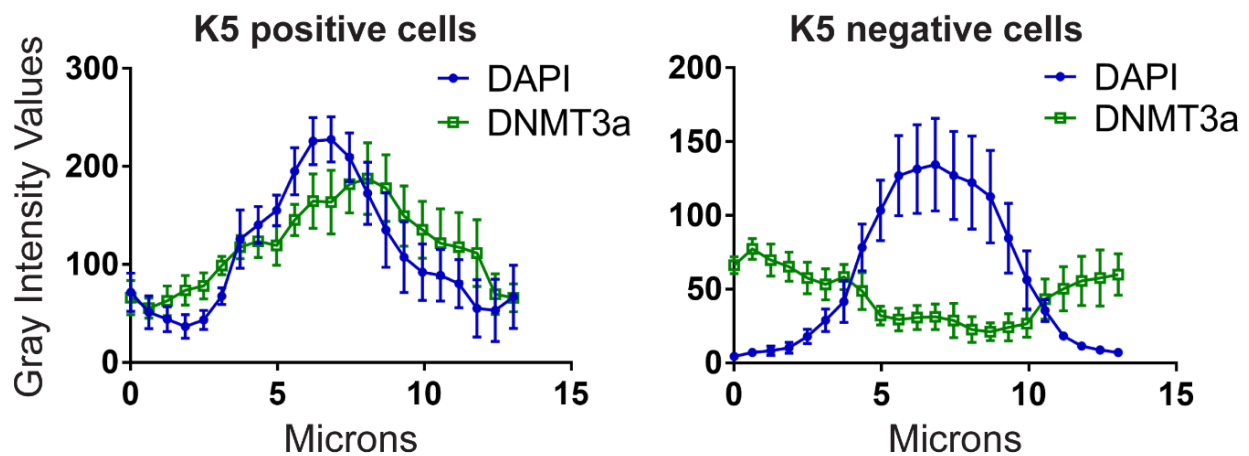
A.

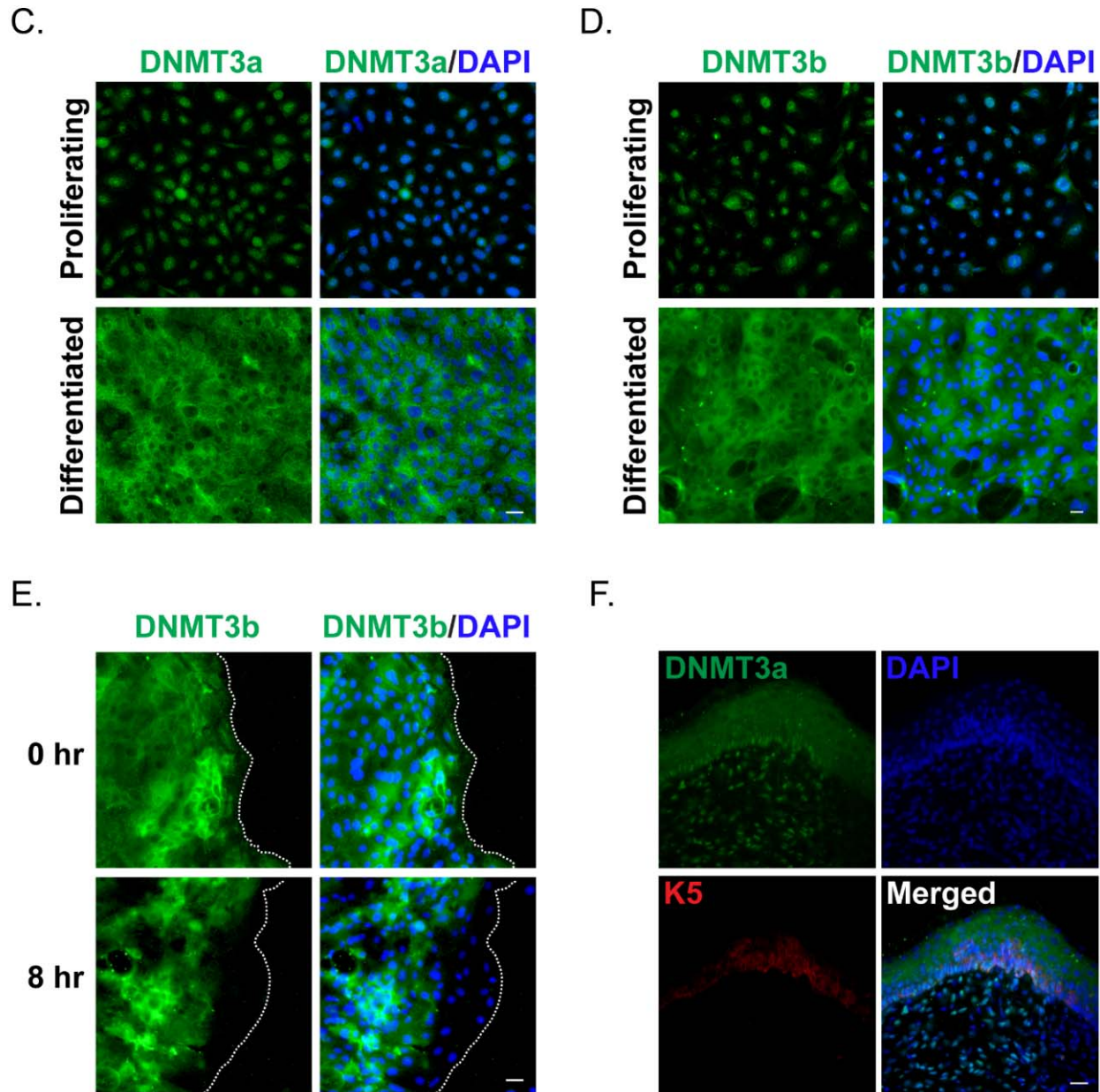


B'.



B''.





209

210 **Figure S2: A**, Representative image of unwounded/wound-distal skin section stained
211 with DNMT3a, DAPI and K5. **B'**, A model showing the quantification method of DAPI
212 and DNMT3a stain intensities over the line of interest (1, 2) from proliferating and
213 differentiated keratinocytes, followed by **B''** the plots of intensity values (gray unit).
214 Staining of in vitro proliferating and differentiated keratinocytes with **C**, DNMT3a/DAPI
215 and **D**, DNMT3b/DAPI. **E**, DNMT3b/DAPI staining of scratch wounded in vitro

216 differentiated keratinocytes. **F**, DNMT3a, DAPI and K5 staining of a completely healed
217 mouse skin section [scale = 20 μ m]

218 **DNMT3a directly regulates caspase-8 expression**

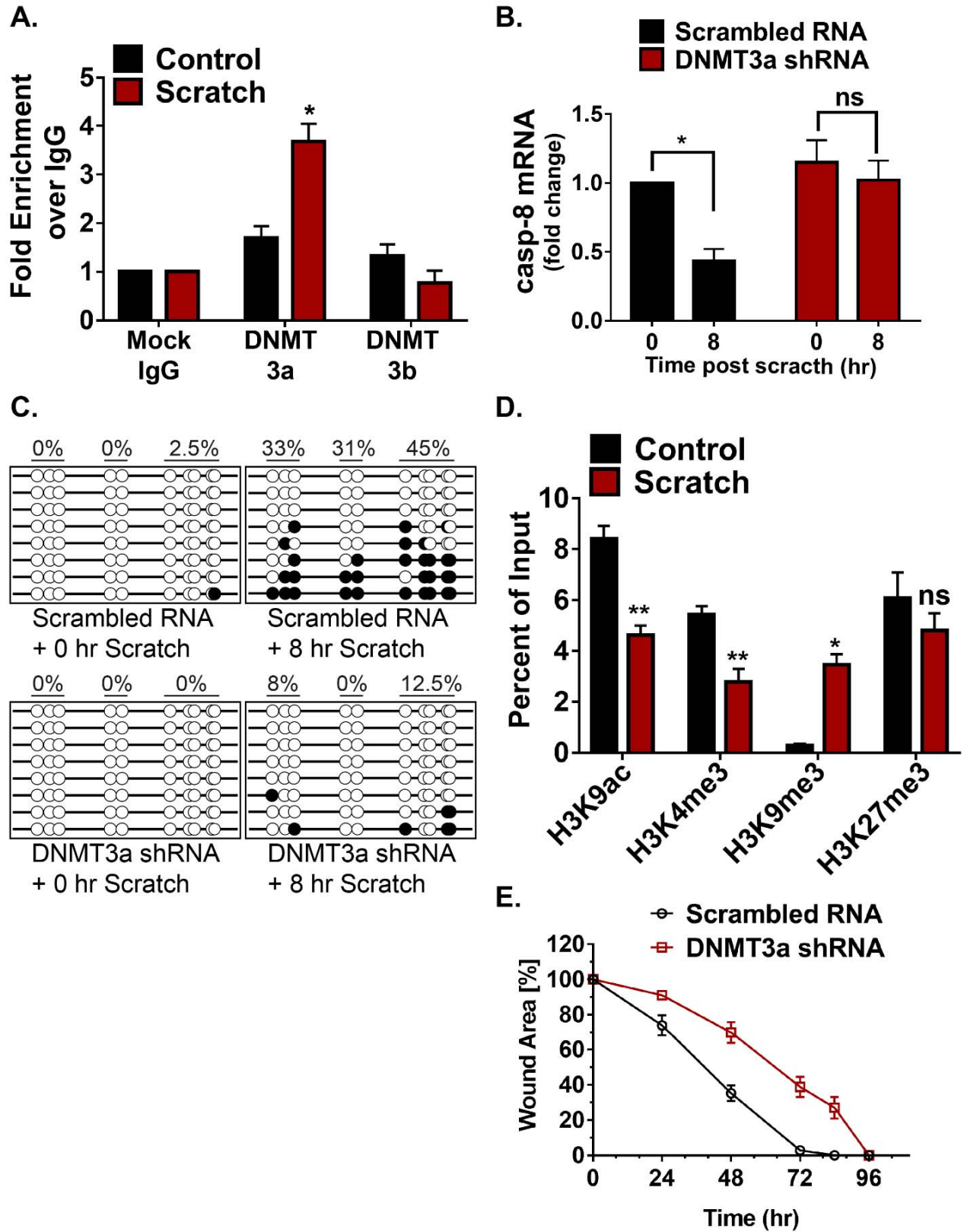
219

220 We further explored whether the de-novo DNA methylation of caspase-8 promoter is the
221 result of DNMT3a's direct binding to this region (Figure S1B). This was accomplished
222 with the use of Chromatin Immunoprecipitation (ChIP) to assess the level of DNMT3a
223 occupancy on the caspase-8 promoter pre- and post-scratch wound. We found that
224 scratch wounds lead to the higher occupancy of DNMT3a on caspase-8 promoter,
225 which is not seen in the case of DNMT3b (Figure 3A). To understand the functional
226 relevance of DNMT activity in maintaining caspase-8 levels, we pre-treated the
227 differentiated keratinocytes with a generic DNMT inhibitor (5-Aza-2'-deoxycytidine). We
228 observed that the inhibitor treated cells were unable to downregulate caspase-8 mRNA
229 in a scratch wound assay (Figure S3A). To specifically assess the role of DNMT3a, we
230 performed shRNA mediated knockdown of DNMT3a (Figure S3B). Compared to the
231 scrambled RNA controls, keratinocytes with reduced DNMT3a expression were unable
232 to downregulate caspase-8 in response to scratch wound (Figure 3B). We further
233 analysed whether failure of caspase-8 mRNA downregulation was due to the absence
234 of promoter methylation. Indeed, scratch-wounded keratinocytes, transduced with
235 DNMT3a shRNA, showed significantly reduced DNA methylation pattern on the
236 caspase-8 promoter compared to scrambled RNA control (Figure 3C).

237

238 Promoter activities are often dependent on the associated histone modifications. These
239 histone marks generally guide the DNA methylation at a particular genic region and
240 vice-a-versa(21–23). DNMT3a occupancy and activity has also been shown to be
241 influenced by the methylation status of certain lysine (K) residues on the histone 3 (H3)
242 tail(22, 24). To investigate the core machinery required for DNMT3a mediated
243 methylation on the caspase-8 promoter, we assessed several activation and repression
244 histone marks in scratch wounded keratinocytes (Figure 3D). We observed that two
245 transcriptional activation marks, H3K9ac and H3K4me3, are decreased at the caspase-
246 8 promoter. On the other hand, the H3K9me3 mark, which is associated with
247 transcriptional repression, was significantly increased at the caspase-8 promoter
248 following wounding. Interestingly, another classical repressive mark, H3K27me3, did not

249 show a significant change. It is possible that the caspase-8 proximal promoter is
250 another example of a bivalent promoter (25) having both activation (H3K9ac and
251 H3K4me3) and repression (H3K27me3) marks. In this scenario, then, wound-mediated
252 repression of caspase-8 is achieved via reduction of both H3K9ac and H3K4me3 along
253 with an increase in the H3K9me3 mark and DNMT3a occupancy. These results
254 establish the mechanism by which DNMT3a localizes to the caspase-8 promoter. An
255 outstanding question is whether DNMT3a is required for a proper wound healing
256 response. To address this issue, we tested the effect of the knockdown of DNMT3a in a
257 scratch wound assay (Figure 3E). We found that keratinocytes with decreased
258 DNMT3a exhibited an impaired wound closure response, thereby illustrating the
259 necessity of this methyltransferase in the proper repithelialization of an in vitro wound.



261

262 **Figure 3: Involvement of DNMT3a and histone modification in regulating caspase-**

263 **8 expression: A**, ChIP-qPCR analysis to check DNMT3a and DNMT3b occupancy at

264 caspase-8 promoter in control and scratch-wounded keratinocytes (n=3) **B**, qPCR

265 analysis of caspase-8 mRNA in scratch-wounded keratinocytes, transduced with either

266 scrambled RNA or DNMT3a shRNA (n=3) **C**, DNA methylation status of caspase-8

267 promoter in scratch-wounded keratinocytes, transduced with either scrambled RNA or

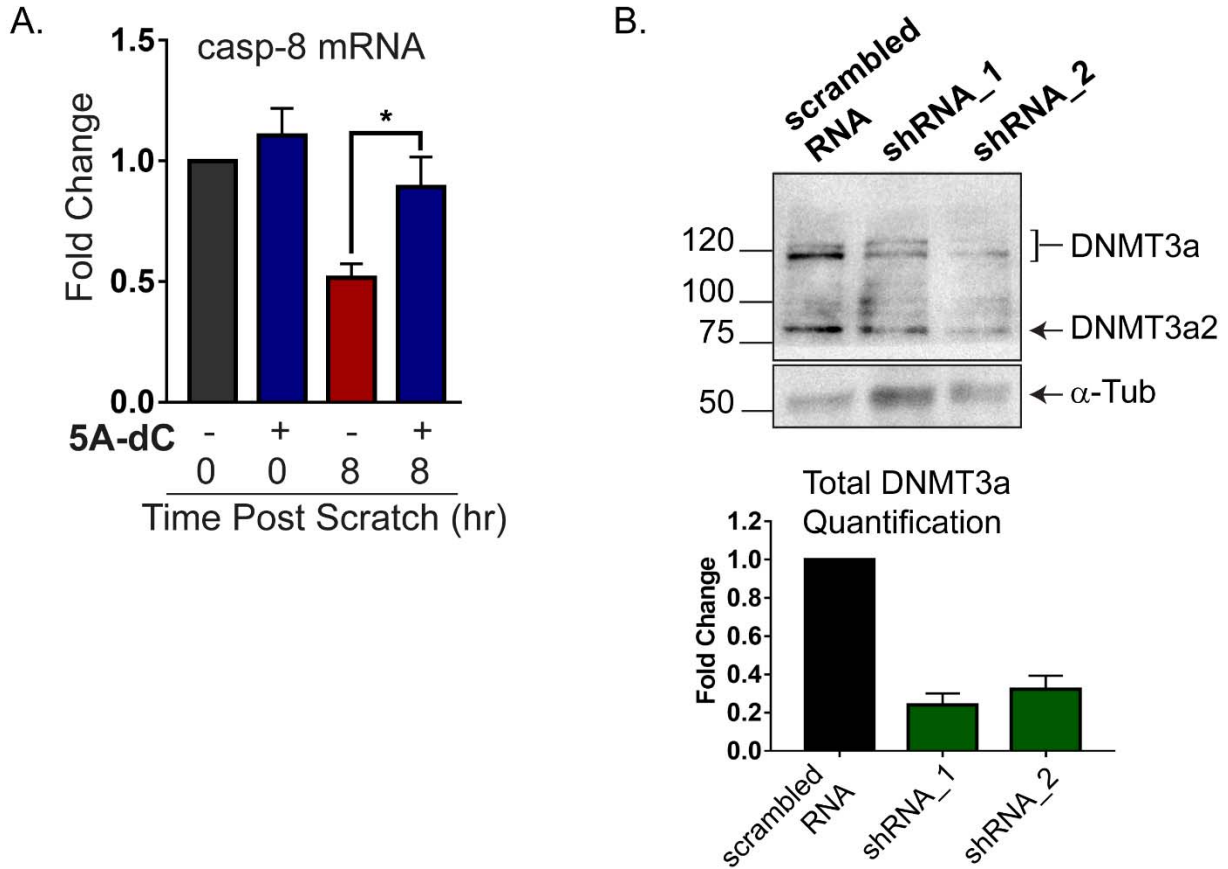
268 DNMT3a shRNA **D**, ChIP-qPCR analysis of H3K9ac, H3K4me3, H3K9me3, and

269 H3K27me3 at caspase-8 promoter in control and scratch-wounded keratinocytes (n=3)

270 **E**, Effect of DNMT3a downregulation on in vitro wound healing assay (Data are shown

271 as mean \pm SEM, P values were calculated using two tailed t-test (A, B, D), * P \leq 0.05,

272 ** P \leq 0.01, *** P \leq 0.001, ns = P > 0.05)



273

274 **Figure S3: A**, qPCR analysis of caspase-8 mRNA in scratch-wounded keratinocytes,
275 pre-treated with 5-Aza-2'-deoxycytidine (5A-dC) or DMSO (n=3) **B**, western blot
276 analysis from keratinocytes transduced with scrambled RNA or DNMT3a shRNA (α -Tub
277 = alpha-tubulin) (Data are shown as mean \pm SEM, P values were calculated using two
278 tailed t-test (A), * P \leq 0.05, ** P \leq 0.01, *** P \leq 0.001, ns = P > 0.05)

279 **Effect of cellular tension on DNMT3a localization and caspase-8 expression**

280

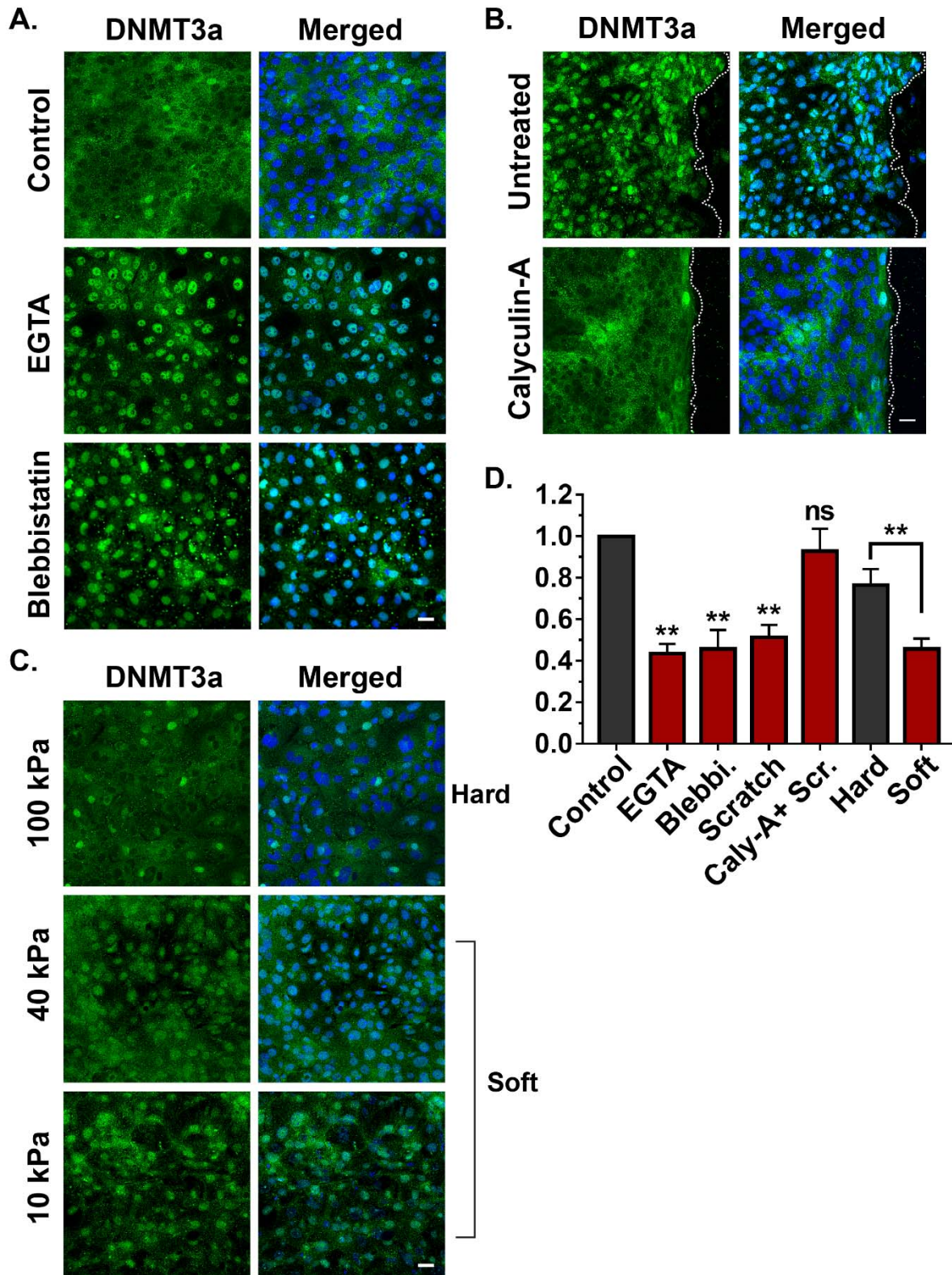
281 We observed that caspase-8 downregulation and DNMT3a nuclear localization initiate
282 at the edge of wound site (Figure 1, 2). Given that these are early responses to injury,
283 understanding the mechanistic basis of this phenomena can provide insights into the
284 broader process of cellular wound sensing. The keratinocytes in the epithelial sheet are
285 strongly connected to each other and an event of injury will result in the sudden
286 relaxation in that tension, particularly in the cells at the boundary of the wound.
287 Interestingly the expanding number of cells exhibiting the downregulation of caspase-8
288 RNA in the scratch wound assay over time (Figure 1A) closely parallels the changes in
289 traction force previously reported for the collective cell migration of an epithelial sheet
290 following a scratch wound (26). We therefore investigated whether release of tension,
291 caused by the severing of the epithelial sheet, can impact DNMT3a subcellular
292 localization and subsequently caspase-8 expression. As shown in Figure S4a,
293 modulation in cellular tension can be achieved via targeting the components of the
294 adherens junction, which are known to play a role in generating and maintaining cellular
295 tension (27, 28).

296 We observed that tension release by disrupting calcium-dependent E-cadherin junctions
297 via EGTA treatment resulted in the nuclear localization of DNMT3a (Figure 4A).
298 Similarly, releasing cellular tension endowed by Non Muscle Myosin II (NM-II) with the
299 pharmacological inhibitor of NMII, blebbistatin, induced the DNMT3a's nuclear
300 translocation from the cytosol (Figure 4A). Furthermore, we examined the effect of
301 blocking release of cellular tension in a scratch wounded sheet of epidermal
302 keratinocytes. The release of tension was blocked by pre-treating keratinocytes with
303 calyculin-A, which inhibits myosin light chain phosphatase, thereby maintaining the
304 active state of NMII (29). The treatment of keratinocytes with calyculin-A prior to
305 scratch wounding blocked the nuclear translocation of DNMT3a that was observed in
306 cells treated with vehicle control (Figure 4B).

307 In addition to a pharmacological approach, we also modulated cellular tension by
308 altering the substrate stiffness on which the keratinocytes were growing. This was
309 accomplished by utilizing polyacrylamide gels of various stiffness, which would alter

310 cellular tension. We observed that differentiated keratinocytes seeded on “soft” matrices
311 ranging from 10 kPa to 40 kPa mostly harboured DNMT3a in the nuclei (Figure 4C).
312 However, cells grown on a “stiffer” matrix (100kPa) predominantly showed a
313 cytoplasmic localization of DNMT3a.
314 We then evaluated whether DNMT3a’s dynamic localization in response to
315 pharmacological and mechanical alterations in cellular tension has any transcriptional
316 consequences. We observed that in all the scenarios where DNMT3a nuclear
317 localization was favored (scratch wounds, EGTA/blebbistatin treatment, soft substrates),
318 caspase-8 RNA was downregulated compared to their respective controls (Figure 4D).
319 On the otherhand, inhibition of DNMT3a’s nuclear localization (via calyculin-A, or a stiff
320 substrate) resulted in the failure of caspase-8 downregulation in spite of a scratch
321 wound. These results suggest that keratinocytes organized within an epithelial sheet
322 can translate changes in tensile forces into cellular reprogramming via epigenetic means.

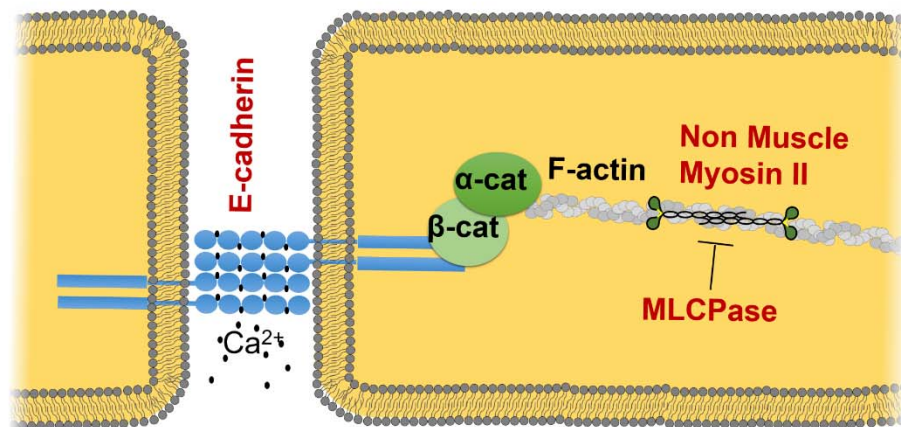
323



324

325 **Figure 4 Effect of cellular tension on DNMT3a localization and caspase-8**
326 **expression: A, Effect of EGTA and Blebbistatin on the localisation of DNMT3a B,**
327 **Effect of scratch wound DNMT3a localisation in presence and absence of calyculin-A**
328 **C, Effect of various matrix stiffness on the localisation of DNMT3a D, Fold change in the**
329 **levels of caspase-8 mRNA as a result of various pharmacological and mechanical**
330 **approaches of tension modulation (n=3), [scale bar = 20 μ m] (Data are shown as**
331 **mean \pm SEM, P values were calculated using two tailed t-test (D), * P \leq 0.05, ** P \leq**
332 **0.01, *** P \leq 0.001, ns = P > 0.05)**

333
334
335
336
337



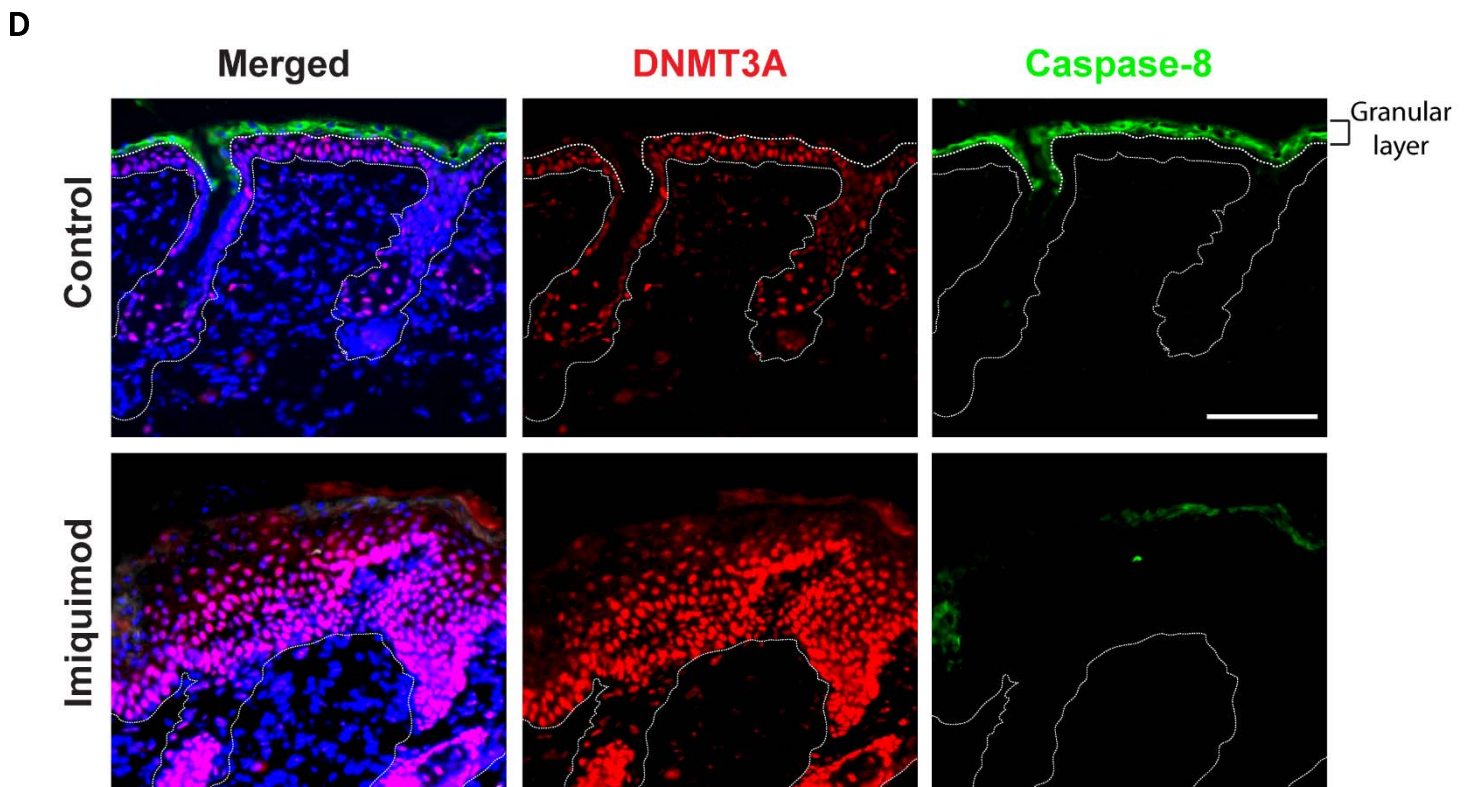
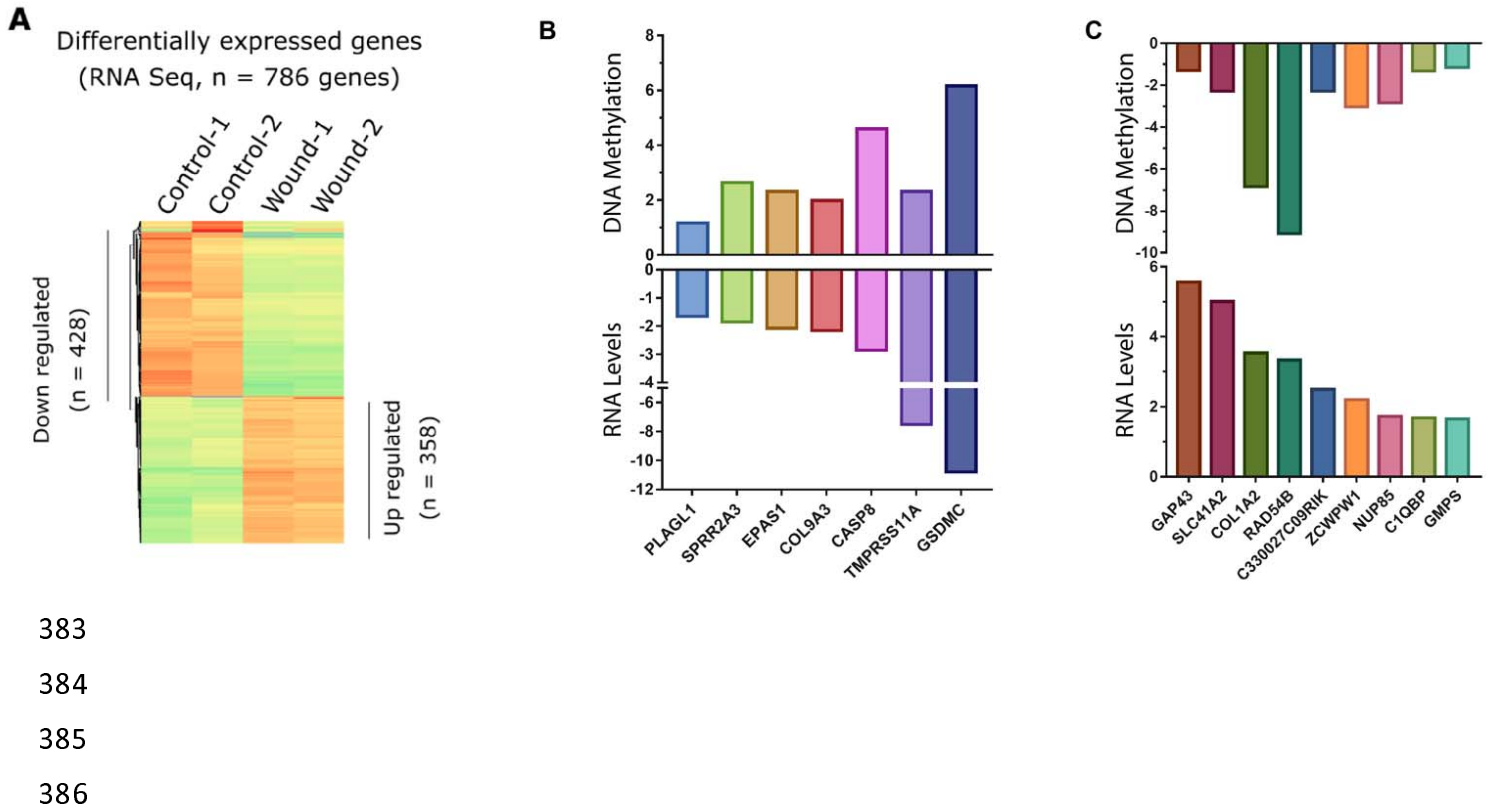
338
339 **Figure S4:** Model showing various potential protein molecules (red labels) involved in
340 generating and/or sensing the cellular tension

341 **DNA methylation could be a global regulator of gene expression to initiate**
342 **wound-healing program**

343
344 We further assessed whether the downregulation of caspase-8 is a paradigm for the
345 global downregulation of genes to achieve a cell state transition from homeostasis to
346 wound healing. Surprisingly, the transcriptome profile of scratch wounded
347 differentiated keratinocytes has not been reported even though these layers are the first
348 to encounter damage in vivo. Thus we performed RNA sequencing of wounded v/s
349 unwounded primary mouse keratinocyte that were differentiated via the calcium switch
350 protocol (Figure 5A). The analysis of the transcriptome data revealed that the number
351 of downregulated genes outnumbered the upregulated genes post injury. We verified
352 the sequencing data by specifically analysing genes via qPCR that have already been
353 implicated in wound healing or epidermal development (Figure 5B and C). Interestingly,
354 there was an inverse correlation with the RNA expression and the degree of methylation
355 for many of the genes we interrogated. This suggest that DNA methylation could be a
356 global regulator for a set of wound response genes (in addition to caspase-8), needed
357 for the wound healing program.

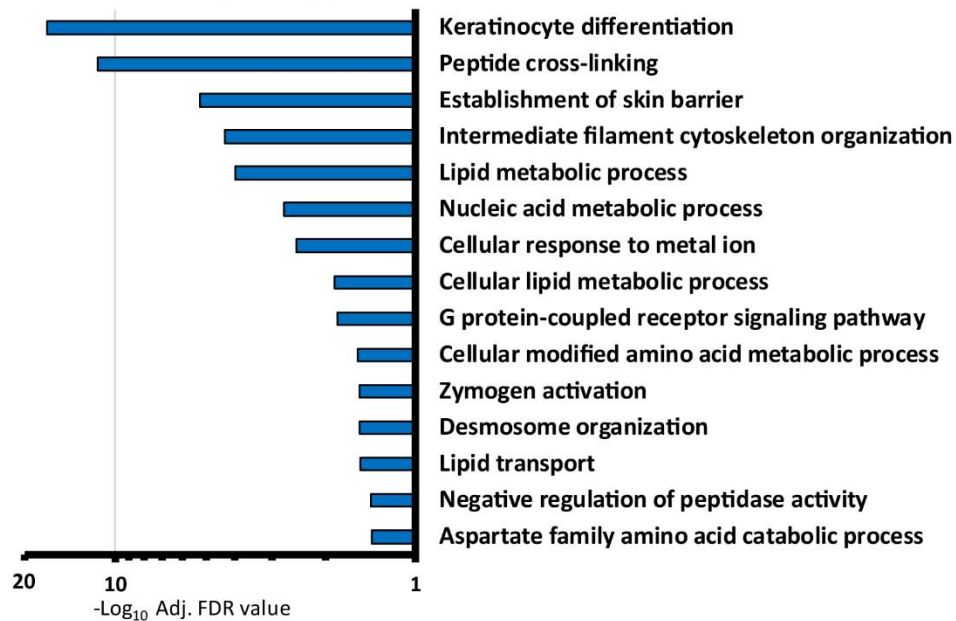
358 Analysis of transcriptome data has revealed many such group of genes and their
359 biological processes. (Figure S5). Of particular interest were the downregulation of
360 genes involved in the differentiation of keratinocytes. The Ghazizadeh lab has reported
361 evidence of dedifferentiation of suprabasal keratinocytes as a mode of aiding cutaneous
362 regeneration and repair. Interestingly, the regeneration of skin epithelia by differentiated
363 epidermal cultures was found to be facilitated by the capacity of these cells to proliferate
364 (30). The transcriptome profile of scratch wounded differentiated keratinocytes reveals
365 an upregulation of cell cycle associated genes that is consistent with this report.
366 Consequently, the convergence of mechanical and epigenetic cues appears to play an
367 important role in the plasticity of differentiated epidermal keratinocytes in cutaneous
368 repair and regeneration. The processes that occur during the wound healing phases of
369 inflammation, proliferation, and tissue remodeling are often reproduced in a deregulated
370 manner in many pathologies leading to the notion of diseases with a “wound signature”.
371 Prominent among these is the view of cancer as an overhealing wound (31). As we

372 noted earlier, there is a body of literature demonstrating that the downregulation of
373 caspase-8 in cancer cells is accompanied with the methylation of its promoter region
374 (32–35). In addition, we have previously demonstrated that inflammatory human skin
375 diseases such as atopic dermatitis (15) and psoriasis (16) likewise exhibit a loss of
376 epidermal caspase-8. To probe a possible link between caspase-8 downregulation and
377 methyltransferase expression, we utilized the imiquimod-induced model of psoriasis in
378 mice. In the psoriatic skin of mice, we observed robust nuclear localisation of DNMT3a
379 in all the epidermal layers, whereas in the control animals, nuclear DNMT3a was
380 primarily localized in the basal keratinocytes (Figure 5D). Altogether, this suggests that
381 the epigenetic regulation governing the cell state transition in wound healing is usurped
382 in many diseases ranging from inflammatory skin diseases to carcinomas.

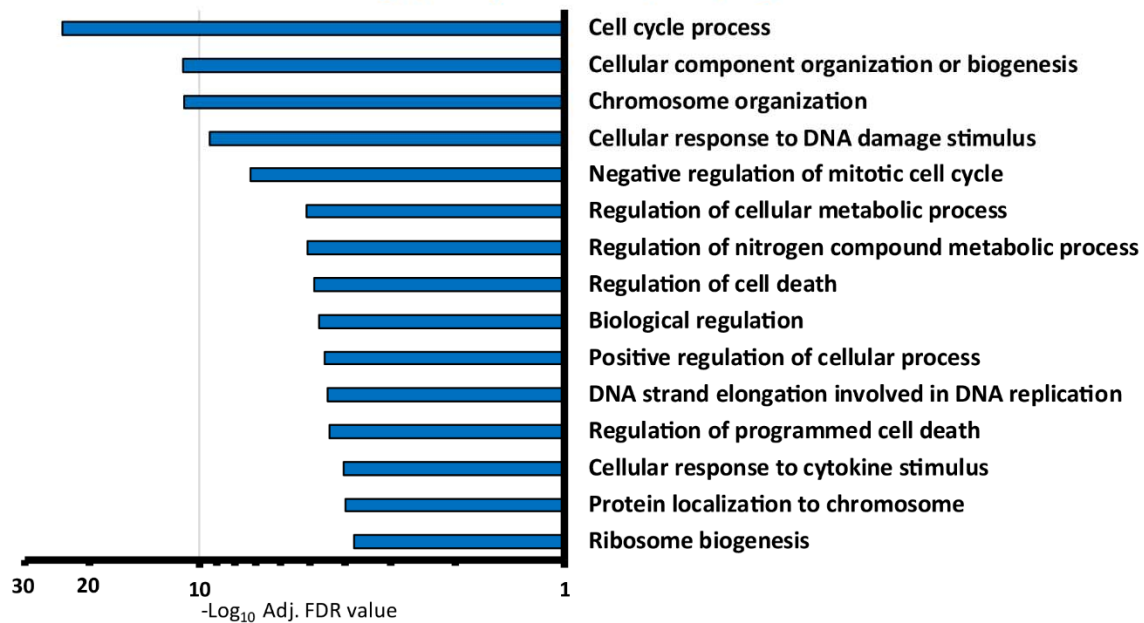


387 **Figure 5: A**, Heat map of differentially regulated genes in Control and Scratch wounded
388 keratinocytes. **B**, Transcriptionally downregulated genes and their associated DNA
389 methylation levels **C**, Transcriptionally upregulated genes and their associated DNA
390 methylation levels. (MeDIP-qPCR, y-axis = fold change compared to control) **D**,
391 DNMT3a and caspase-8 staining of Control and Psoriatic mouse skin (induced through
392 imiquimod treatment). [scale bar = 100 μ m]

Gene Ontology (Biological Process) of Downregulated Genes



Gene Ontology (Biological Process) of Upregulated Genes



393

394 **Figure S5:** Gene ontology of Upregulated and Downregulated genes (Biological
395 Processes). Processes are listed as $-\log_{10}$ of adjusted FDR values. Top 15 relevant
396 biological processes are chosen for generating the graphs.

397 **DISCUSSION**

398 The wound-healing literature involving epidermal keratinocytes have elegantly
399 described many signaling pathways and gene expression profiles in the proliferating
400 cells of the basal layer (36, 37). In contrast, differentiated epidermal cells, such as the
401 suprabasal keratinocytes near the outer surface of the skin, have largely been
402 overlooked for their potential role during wound-healing. Interestingly, our previous
403 work demonstrates that the uppermost layer of differentiated keratinocytes, namely the
404 granular layer, expresses caspase-8 that has a non-canonical role in regulating the
405 wound-healing program (12). It was found that the downregulation of caspase-8 is both
406 necessary and sufficient to induce a wound healing response in the absence of any
407 tissue damage. In addition, the chronic downregulation of caspase-8 underlies
408 inflammatory skin diseases such as atopic dermatitis (15) and psoriasis (38). These
409 findings have made the decrease in caspase-8 expression a useful wound-healing
410 biomarker and led us to inquire about the mechanism of caspase-8 regulation in skin
411 keratinocytes.

412 Clues about the regulation of caspase-8 is reported in the context of cancer. Similar to
413 the wound-healing process, it is generally downregulated in various cancers (18, 39,
414 40). It is possible that the cancers, known as “over healing wound”, usurp physiological
415 pathway of wound-healing for its own propagation (31). Here we show that wound-
416 sensing leads to the acute increase in the caspase-8 promoter methylation as a
417 potential mechanism of gene silencing. This parallels with the findings on caspase-8
418 downregulation in hepatocellular carcinoma, where methylation status of SP1 sites and
419 nearby CpG dinucleotides in the promoter region were proposed to be a major regulator
420 of caspase-8 expression (19). In fact, it has been observed that caspase-8 and several
421 other genes are known to be downregulated in various cancers via DNA
422 methyltransferase (DNMT) activity (18, 39, 40). The overexpression of DNMT3a has
423 also been shown to be associated with several cancers (41, 42)The process of de-novo
424 DNA methylation during an acute physiological response such as wound healing is a
425 rarely described phenomenon. Mammalian cells are known to have only two de-novo
426 DNA methyltransferases, DNMT3a and DNMT3b. Both have been widely studied for
427 their role in physiological processes like embryogenesis (43) and hematopoiesis (44),

428 as well as pathological conditions such as cancer (45, 46). In particular, , it has been
429 shown that DNMT3a and 3b are required as regulators of enhancer activity and RNA
430 production of genes necessary for epidermal stem cell homeostasis (4). In disease
431 context, DNMT3a has been described to be overexpressed or mutated in various
432 carcinomas (47, 48) and correlates with the downregulation of caspase-8 in these same
433 scenarios. Here, we found that upon injury to the skin or differentiated epidermal
434 sheets, the suprabasal cells near wound edge showed a nuclear localization of
435 DNMT3a, but not DNMT3b. We have captured that DNMT3a indeed occupies the
436 caspase-8 promoter and plays an important role in its downregulation post injury. In
437 parallel to the DNA methylation, the literature also describes changes in histone
438 modifications responsible for the ON/OFF state of a particular gene. The histone
439 modifications and their modifiers have been studied in depth to understand how the
440 expression of various epidermal differentiation genes are regulated (49). In general,
441 H3K9ac, H3K4me3 are considered as gene activation marks and H3K9me3 and
442 H3K27me3 are known as repression mark. It is also observed that certain methylation
443 state of H3K36 dictates the DNMT3a's recruitment to a particular DNA segment on the
444 chromosome (50, 51). In our efforts to understand the histone modifications during
445 wound-healing, we observed a reduction in H3K9ac and H3K4me3 levels, along with an
446 increase in the H3K9me3 mark at the caspase-8 promoter. These histone modifications
447 are known to be regulated via various other epigenetic players such as Polycomb
448 repressive complexes (PRC 1/2), JMJD, Setd8, and HDACs during epidermal
449 development (49).

450 How these epigenetic players are regulated is another important question in the field.
451 While there are many chemical cues, adhesion signals, and transcription factors
452 described to regulate the wound-healing process, emerging evidence links mechanical
453 forces to epigenetic and transcriptional responses (52, 53). Even during the
454 development of epidermal tissue, tension generating molecular players like non-muscle
455 myosin IIA (NMIIA), along with emerin (Emd) and PRC2 regulate the differentiation
456 process of epidermal stem cells. The strain on epidermal cells reduces Emd levels from
457 the inner nuclear membrane, which then leads to the loss of the histone mark
458 H3K9me2,3. This is followed by Polycomb repressive complex 2 (PRC2) mediated

459 increase of H3K27me3 occupancy at several heterochromatic regions and thereby gene
460 silencing (54). Along the same line, recently Nava et al. has described how short and
461 long term mechanical stress on a cell can result in changes in stiffness of the nuclear
462 membrane, loss of H3K9me3 marks at the heterochromatin and overall chromatin and
463 cytoskeletal reorganization (55). These are some of the key discoveries suggesting
464 external mechanical forces drive changes in heterochromatin organization, gene
465 expression changes, and cytoskeletal reorganization in a way that mechanical energy
466 gets redistributed and DNA damage can be avoided. In this context, our results
467 demonstrate that the release in the mechanical tension, either by physical or chemical
468 treatments, results in the DNMT3a's nuclear localization and downregulation of
469 caspase-8. This observation is consistent with the concept of mechano-sensitive
470 histone modifications, which could lay a foundation for the occupancy of DNMT3a. In a
471 wider context of cellular reprogramming during the wound response,
472 mechanotransduction seem to have a large impact on the transcriptome of the cell via
473 the concomitant initiation of several epigenetic pathways. Future studies in this area will
474 include elucidation of the connection between the release of mechanical tension and
475 their sensing by these epigenetic machineries. For example, DNMT3a has been shown
476 to have multiple binding partners (DNMT3L, SUMO-1, Cbx4, Ubc9, RP58, HDAC1) for
477 their nuclear shuttling as well as chromosomal occupancy, some of which can
478 potentially function as a primary signal sensor to guide the localization of DNMT3a (56,
479 57). Moreover, in different cell types, changes in mechanical tension have been
480 documented to directly induce the nuclear translocation of important transcription
481 factors. A notable example of which is the YAP/TAZ complex, which has proliferation
482 stimulating gene targets (58).

483 The described model of mechanosensitive epigenetic players would obviously be
484 regulating a larger gene regulatory network, in addition to caspase-8. Interestingly the
485 transcriptome literature on wound-healing has utilized proliferating keratinocytes,
486 leaving the transcriptome profile of differentiated keratinocytes unknown despite the fact
487 that it constitutes about 2/3 of the epidermis. Our research fills an important gap by
488 providing a transcriptome profile of in vitro wounded differentiated keratinocytes. The
489 results give us a unique insight in the regulation of various unexplored wound-response

490 genes. On a particular note, we observe a strong downregulation of multiple epidermal
491 differentiation genes in response to injury. From the current transcriptome and literature
492 survey it is evident that various keratinocyte differentiation markers (such as involucrin,
493 keratins K1/K10, and filaggrin) are downregulated along with cell adhesion molecules
494 (involved in tight junction, adherens junctions, and desmosomes). This is consistent
495 with a report from S. Ghazizadeh's lab that de-differentiation of suprabasal
496 keratinocytes is a contributing factor in the wound healing response (30). Our data
497 suggests that the release of mechanical tension in differentiated keratinocytes is one
498 component in this process by inducing a "partial de-differentiation" and perhaps
499 additional soluble signaling cues are required to achieve complete dedifferentiation.

500 **Materials and Method:**

501

502 **Cell culture and scratch wound assay:**

503

504 The isolation of primary keratinocytes from neonatal mice was performed as described
505 in (59). Briefly, mice pups were sacrificed and the skin was removed. The skin was kept
506 in dispase at 4° C overnight (or 37 ° C for 1 hour) to separate epidermis. The epidermis
507 was then digested with trypsin to isolate keratinocytes. These cells were filter with 70-
508 micron mesh and cultured further as described in (Novak et al. 2009) (60). The
509 keratinocytes were cultured in lab with feeder cells (3T3J2) for 10 passage. Then feeder
510 independent keratinocytes were taken and tested for their differentiation potential via
511 calcium switch protocol (61). Various differentiation markers were checked via qPCR.
512 The batch of cells showing proper differentiation and morphology were then selected for
513 further experiments.

514 Proliferating keratinocytes were maintained in low Ca²⁺ E-media (0.05mM). For
515 differentiation they were allowed to reach 100% confluence and then introduced with
516 high Ca²⁺ (1.2mM) E-media for 48 hrs. Once they differentiated and appear as sheet-
517 like morphology, scratch-wounds were made (with the help of a 1ml tip) at multiple sites
518 in each culture plate. To keep the constancy between experiments, the distance
519 between the consecutive scratch was kept approximately 0.5 mm. The scratch wounds
520 were followed by a 1X PBS wash, and fresh high Ca²⁺ (1.2mM) E-media were added to
521 each plate. As described in the figure legends, the cells were harvested at several time
522 points using TRIzol reagent for RNA isolation or using lysis buffer for DNA isolation.

523

524 **Mice:**

525

526 C57Bl6/J animals were originally purchased from Jackson Laboratory (Stock No.
527 000664) and were bred for > 10 generations in the NCBS vivarium facility. 8-week-old
528 mice were anesthetised and 5 mm or 8 mm punch biopsies were used to make full-
529 thickness excisional wounds.

530

531 **Tissue Section and Staining:**

532

533 Wounded regions were embedded in OCT, frozen on dry ice, and stored in -80° freezer
534 for further sectioning and antibody staining. 10-15 micron section were taken, stained
535 with primary antibody at 4° C overnight, and then with secondary antibody at RT for 20-
536 30 minutes. Antibodies used in this study are as following; Caspase-8 (Enzo #ALX-804-
537 447-C100), DNMT3a (abcam #ab2850, SC #365769), K5 (lab generated). Sections
538 were imaged using IX73 Olympus microscope.

539

540 **In-situ hybridisation:**

541

542 DIG labelled 5' mouse caspase-8 cRNA probe was synthesized as per the
543 manufactures instructions (Roche dig labelling kit – # 11175025910). In situ
544 hybridisation was performed as described earlier (62). Briefly, the paraffin tissue
545 sections were deparaffinised by treatment by xylene and ethanol gradient, or the
546 4%PFA fixed cells were permeabilized using 0.2% TritonX-100 for 10 minutes at room
547 temperature. 5ng DIG labelled cRNA probes per 100uL hybridisation buffer was applied
548 on the sections overnight at 63°C. Same concentration of DIG labelled mRNA with the
549 complimentary sequence to cRNA was used as a negative control. Washing was done
550 at 65°C. The Anti-DIG antibody (Roche # 11093274910 Roche) was applied overnight
551 as per manufacturer's instructions. Sections were developed for 30 minutes at 37°C
552 using BCIP/NBT solution (Sigma # B6404). Reaction was stopped using de-ionised
553 water once the purple colour was developed. Sections were mounted using MOWIOL
554 solution and imaged using bright-field microscope.

555

556 **Hydrogel of varying stiffness:**

557

558 The polyacrylamide based hydrogels were prepared as describe in (63) and (64). They
559 were coated with collagen and seeded with enough cells to make it 80-100% confluent,
560 and were allowed to settle for 24-48 hr before initiating the keratinocyte differentiation.

561

562 **Chromatin Immunoprecipitation (ChIP):**

563

564 ChIP of histone modification was performed as described previously (65) with some
565 modifications. In brief, harvested keratinocytes (unscratched and scratched) were
566 cross-linked with 1% formaldehyde. Cells were lysed in buffer N containing DTT,
567 PMSF, and 0.3% NP-40. After isolation of nuclei, chromatin fractionation was done
568 using 0.4 U of MNase (N5386, Sigma) at 37°C for 10 min. Reaction was stopped using
569 MNase stop buffer without proteinase K. Simultaneously, antibodies against
570 H3K27me3, H3K9me3, H3K4me3, H3K9ac and Rabbit IgG were kept for binding with
571 Dynabeads for 2 hr at RT. After equilibration of beads, chromatin was added for
572 pre-clearing. To antibody bound beads, pre-cleared chromatin was added and kept for
573 IP at 4°C overnight. Next day, beads were washed and eluted at 65°C for 5 min. Eluted
574 product was subjected to reverse cross-linking along with input samples, first with
575 RNase A at 65°C overnight and then with Proteinase K at 42°C for 2 h. After reverse
576 cross-linking, DNA purification was performed using phenol:chloroform extraction
577 method. Antibodies used for this protocol are listed here:

<i>Antibody</i>	<i>Cat #</i>	<i>Company</i>
H3K27me3	07-449	Millipore
H3K9me3	ab8898	abcam
H3K9ac	ab4441	abcam
H3K4me3	ab8580	abcam

578

579 **Bisulphite reaction, sequencing, and analysis:**

580

581 Genomic DNA was isolated by salting out method as described elsewhere (66), then
582 treated with RNase for 1 hour at 37° C. Further, ~ 20 microgram DNA was taken in 200
583 microliter volume and purified with phenol:chloroform extraction method. The purified
584 DNA was checked for its integrity via running on the agarose gel. The DNA sample
585 having good integrity and free of RNA were taken for bisulphite conversion as per
586 manufacturer's protocol (Zymo #D5005). The converted DNA was then amplified using

587 bisulphite conversion specific primers, the amplified product was assessed on the
588 agarose gel, ligated with TOPO-TA vector.

589 and then sent for Sanger's sequencing. caspase-8 promoter - for bisulphite
590 sequencing (GAATAAGGAAGTGTTTTTTAG, AAAACTATACTCACTTCCTATTC). The
591 sequenced file (FASTA) was uploaded to <http://quma.cdb.riken.jp/> for CpG methylation
592 analysis.

593

594 **Lentivirus shRNA constructs and transduction:**

595

596 Plasmids expressing shRNAs were obtained from TransOmics (DNMT3a #
597 TLMSU1400). To produce viruses, HEK293T cells were transfected with psPAX2,
598 pMD2.G, and either non targeting random RNA sequence vector or shRNA- containing
599 plasmids, using Lipofectamine® LTX & PLUS transfection reagents according to the
600 manufacturer's protocol. Following a 48-72 hr transfection, the virus particle-containing
601 media was collected, concentrated with filters, and added to the differentiated cells for
602 24 hr. Expression of DNMT3a was measured two to three days after viral infection.
603 Silencing efficiency was confirmed by immunoblotting.

604

605 **Quantitative Real Time PCR:**

606

607 RNA was isolated from human keratinocytes (proliferating or differentiated) using the
608 RNAiso Plus (Takara). 1 µg of RNA was used to prepare cDNA using the PrimeScript
609 kit (Takara). cDNA equivalent to 100 ng of RNA was used for setting up the qPCR
610 reaction using the SYBR green 2x master mix. All reactions were performed in
611 technical triplicates using the CFX384 Touch Real time PCR detection system (BioRad).
612 Primers used in this study are listed here: caspase-8 mRNA
613 (TCTGCTGGGAATGGCTACGGTGAA, GTGTGAAGGTGGGCTGTGGCATCT),
614 caspase-8 promoter (GGGAATAAGGAAGTGTCCTCCA,
615 CCCAGAACTGTACTCACTTCCTG), beta Actin (GGGCTATGCTCTCCCTCAC,
616 GATGTCACGCACGATTTCC)

617

618 **RNA Sequencing and data analysis:**

619

620 The scratch wounded cells and controls were collected after 8 hours in TRIzol reagent
621 and RNA was isolated using standard TRIzol based RNA isolation method. The library
622 preparation and NGS RNA sequencing steps were outsourced to a commercial facility
623 (Genotypic). Once the raw sequencing reads were received, sequencing data analysis
624 was performed using the following analysis pipeline. Briefly, raw sequencing data was
625 QC checked with the “FASTQC” tool (Babraham Bioinformatics). Adapter contamination
626 and bad quality reads were trimmed using “Trimmomatic” tool (67). The good quality
627 reads were then mapped to mm10 (mouse) reference genome using “HISAT2” (68).
628 The resulting “SAM” outputs were converted to “BAM” output and sorted. The “HTSeq-
629 Count” tool was used to generate expression matrix from all four samples. Then,
630 differential expression was analysed with the help of DESeq2 R package.

631

632 **Gene Ontology Enrichment Analysis:**

633

634 To explore enrichment of Gene Ontology among the significantly down regulated (n =
635 428) and up regulated genes (n = 358) we have used <http://geneontology.org/> resources
636 which runs “PANTHER” for the enrichment analysis (69).

637 Additional details of the NGS RNA seq samples are given here:

Sample Names	Raw Sequencing read counts	Good quality read counts (Used for mapping to mm10 reference genome)	638
Control-1	33693828	30441624	639
Control-2	34605485	30973898	640
Scratch-wound-1	32255293	27735961	641
Scratch-wound-2	31056628	27761854	642
			643

644

645

646

647

648 **ACKNOWLEDGEMENTS**

649 The authors would like to thank Prof. Apurva Sarin, Prof. Tapas Kundu, Prof. Sudhir
650 Krishna and Jamora Lab members for their critical review of the work and insightful
651 discussions. This work was supported by grants to C.J. from the Department of
652 Biotechnology of the Government of India (BT/PR8738/AGR/36/770/2013 and
653 DBT/PR32539/BRB/ 10/1814/2019); and inStem Core funds. TB was supported by
654 PhD scholarship from Council of Scientific & Industrial Research (CSIR). We thank the
655 staff of the NCBS Central Imaging and Flow Cytometry Facility (CIFF) for help with
656 image acquisition. Animal work in the NCBS/inStem Animal Care and Resource Center
657 was partially supported by the National Mouse Research Resource (NaMoR) grant #
658 DBT/PR5981 /MED/31/181/2012;2013-2016 & 102/IFD/SAN/5003/2017-2018 from the
659 Indian Department of Biotechnology

660

661

662 **Author Contributions**

663 Conceptualization, T.B. and C.J.; Methodology, T.B., C.J.; Investigation, T.B., R.D.,
664 A.M.H., A.A.K., A.J.P., A.P.D; Writing – Original Draft, T.B., C.J.; Writing – Review &
665 Editing, T.B., C.J.; Funding Acquisition, C.J. and S.R.; Resources, C.J., and S.R.;
666 Supervision, T.B., C.J., S.R.

667

668 **Declaration of Interests**

669 The authors declare no conflict of interest

670

671

672

673

674

675 REFERENCES

676

- 677 1. T. J. Shaw, P. Martin, Wound repair: A showcase for cell plasticity and migration.
678 *Curr. Opin. Cell Biol.* **42**, 29–37 (2016).
- 679 2. M. A. Troester, *et al.*, Activation of Host Wound Responses in Breast Cancer
680 Microenvironment. *Clin. Cancer Res.* **15**, 7020–7028 (2009).
- 681 3. C. J. Lewis, A. N. Mardaryev, A. A. Sharov, M. Y. Fessing, V. A. Botchkarev, The
682 Epigenetic Regulation of Wound Healing. *Adv. wound care* **3**, 468–475 (2014).
- 683 4. L. Rinaldi, *et al.*, Dnmt3a and Dnmt3b Associate with Enhancers to Regulate
684 Human Epidermal Stem Cell Homeostasis (Elsevier, 2016).
- 685 5. Q. Shen, H. Jin, X. Wang, Epidermal Stem Cells and Their Epigenetic Regulation.
686 *Int. J. Mol. Sci.* **14**, 17861 (2013).
- 687 6. D. Orioli, E. Dellambra, Epigenetic Regulation of Skin Cells in Natural Aging and
688 Premature Aging Diseases. *Cells* **7**, 268 (2018).
- 689 7. L. Cooper, C. Johnson, F. Burslem, P. Martin, Wound healing and inflammation
690 genes revealed by array analysis of “macrophageless” PU.1 null mice. *Genome*
691 *Biol.* (2005) <https://doi.org/10.1186/gb-2004-6-1-r5>.
- 692 8. T. Shaw, P. Martin, Epigenetic reprogramming during wound healing: loss of
693 polycomb-mediated silencing may enable upregulation of repair genes. *EMBO*
694 *Rep.* **10**, 881–6 (2009).
- 695 9. A. Totaro, T. Panciera, S. Piccolo, YAP/TAZ upstream signals and downstream
696 responses. *Nat. Cell Biol.* **20**, 888 (2018).
- 697 10. R. Yang, *et al.*, Epidermal stem cells in wound healing and their clinical
698 applications. *Stem Cell Res. Ther.* 2019 101 **10**, 1–14 (2019).
- 699 11. M. Senoo, Epidermal Stem Cells in Homeostasis and Wound Repair of the Skin.
700 *Adv. Wound Care* **2**, 273 (2013).
- 701 12. P. Lee, *et al.*, Dynamic expression of epidermal caspase 8 simulates a wound
702 healing response. *Nature* **458**, 519–23 (2009).
- 703 13. P. Lee, *et al.*, Stimulation of hair follicle stem cell proliferation through an IL-1
704 dependent activation of $\gamma\delta$ T-cells. *Elife* **6** (2017).
- 705 14. S. Ghosh, *et al.*, Extracellular caspase-1 regulates hair follicle stem cell migration

- 706 during wound-healing. *bioRxiv*, 548529 (2020).
- 707 15. C. Li, *et al.*, Development of atopic dermatitis-like skin disease from the chronic
708 loss of epidermal caspase-8. *Proc. Natl. Acad. Sci. U. S. A.* **107**, 22249–22254
709 (2010).
- 710 16. T. Bhatt, *et al.*, Sustained Secretion of the Antimicrobial Peptide S100A7 Is
711 Dependent on the Downregulation of Caspase-8. *Cell Rep.* **29**, 2546-2555.e4
712 (2019).
- 713 17. S. Fulda, Caspase-8 in cancer biology and therapy. *Cancer Lett.* **281**, 128–133
714 (2009).
- 715 18. D. G. Stupack, Caspase-8 as a therapeutic target in cancer. *Cancer Lett.* **332**,
716 133–40 (2013).
- 717 19. C. Liedtke, *et al.*, Silencing of caspase-8 in murine hepatocellular carcinomas is
718 mediated via methylation of an essential promoter element. *Gastroenterology*
719 **129**, 1602–15 (2005).
- 720 20. L. Rinaldi, *et al.*, Loss of Dnmt3a and Dnmt3b does not affect epidermal
721 homeostasis but promotes squamous transformation through PPAR- γ . *Elife* **6**
722 (2017).
- 723 21. M. Lawrence, S. Daujat, R. Schneider, Lateral Thinking: How Histone
724 Modifications Regulate Gene Expression. *Trends Genet.* **32**, 42–56 (2016).
- 725 22. J. Du, L. M. Johnson, S. E. Jacobsen, D. J. Patel, DNA methylation pathways and
726 their crosstalk with histone methylation. *Nat. Rev. Mol. Cell Biol.* **16**, 519–32
727 (2015).
- 728 23. A. D. King, *et al.*, Reversible Regulation of Promoter and Enhancer Histone
729 Landscape by DNA Methylation in Mouse Embryonic Stem Cells. *Cell Rep.* **17**,
730 289–302 (2016).
- 731 24. X. Guo, *et al.*, Structural insight into autoinhibition and histone H3-induced
732 activation of DNMT3A. *Nature* **517**, 640–4 (2015).
- 733 25. P. Voigt, W.-W. Tee, D. Reinberg, A double take on bivalent promoters. *Genes*
734 *Dev.* **27**, 1318–38 (2013).
- 735 26. X. Trepast, *et al.*, Physical forces during collective cell migration. *Nat. Phys.* **5**,
736 426–430 (2009).

- 737 27. T. Lecuit, A. S. Yap, E-cadherin junctions as active mechanical integrators in
738 tissue dynamics. *Nat. Cell Biol.* **17**, 533–539 (2015).
- 739 28. D. E. Leckband, J. de Rooij, Cadherin Adhesion and Mechanotransduction. *Annu.*
740 *Rev. Cell Dev. Biol.* **30**, 291–315 (2014).
- 741 29. B. Jackson, *et al.*, RhoA is dispensable for skin development, but crucial for
742 contraction and directed migration of keratinocytes. *Mol. Biol. Cell* **22**, 593–605
743 (2011).
- 744 30. J. Mannik, K. Alzayady, S. Ghazizadeh, Regeneration of multilineage skin
745 epithelia by differentiated keratinocytes. *J. Invest. Dermatol.* **130**, 388–397 (2010).
- 746 31. M. Schäfer, S. Werner, Cancer as an overheating wound: an old hypothesis
747 revisited. *Nat. Rev. Mol. Cell Biol.* **9**, 628–38 (2008).
- 748 32. E. M, S. L, W. O, S. W, Promoter methylation pattern of caspase-8, P16INK4A,
749 MGMT, TIMP-3, and E-cadherin in medulloblastoma. *Pathol. Oncol. Res.* **10**, 17–
750 21 (2004).
- 751 33. Y. Wu, M. Alvarez, D. J. Slamon, P. Koeffler, J. V Vadgama, Caspase 8 and
752 maspin are downregulated in breast cancer cells due to CpG site promoter
753 methylation. *BMC Cancer* **10**, 32 (2010).
- 754 34. S. Cho, *et al.*, Epigenetic methylation and expression of caspase 8 and survivin in
755 hepatocellular carcinoma. *Pathol. Int.* **60**, 203–211 (2010).
- 756 35. E. Hervouet, F. M. Vallette, P.-F. Cartron, Impact of the DNA methyltransferases
757 expression on the methylation status of apoptosis-associated genes in
758 glioblastoma multiforme. *Cell Death Dis.* **1**, 1–9 (2010).
- 759 36. I. Pastar, *et al.*, Epithelialization in Wound Healing: A Comprehensive Review.
760 *Adv. Wound Care* **3**, 445–464 (2014).
- 761 37. G. K. Patel, C. H. Wilson, K. G. Harding, A. Y. Finlay, P. E. Bowden, Numerous
762 keratinocyte subtypes involved in wound re-epithelialization. *J. Invest. Dermatol.*
763 **126**, 497–502 (2006).
- 764 38. T. Bhatt, *et al.*, Sustained Secretion of the Antimicrobial Peptide S100A7 Is
765 Dependent on the Downregulation of Caspase-8. *Cell Rep.* **29**, 2546-2555.e4
766 (2019).
- 767 39. A. Nakagawara, *et al.*, High levels of expression and nuclear localization of

- 768 interleukin-1 beta converting enzyme (ICE) and CPP32 in favorable human
769 neuroblastomas. *Cancer Res.* **57**, 4578–84 (1997).
- 770 40. D. Subramaniam, R. Thombre, A. Dhar, S. Anant, DNA Methyltransferases: A
771 Novel Target for Prevention and Therapy. *Front. Oncol.* **4**, 80 (2014).
- 772 41. D. He, *et al.*, DNMT3A/3B overexpression might be correlated with poor patient
773 survival, hypermethylation and low expression of ESR1/PGR in endometrioid
774 carcinoma: An analysis of the Cancer Genome Atlas. *Chin. Med. J. (Engl)*. **132**,
775 161–170 (2019).
- 776 42. I. Kataoka, *et al.*, DNMT3A overexpression is associated with aggressive behavior
777 and enteroblastic differentiation of gastric adenocarcinoma. *Ann. Diagn. Pathol.*
778 **44**, 151456 (2020).
- 779 43. J.-Y. Li, *et al.*, Synergistic Function of DNA Methyltransferases Dnmt3a and
780 Dnmt3b in the Methylation of Oct4 and Nanog. *Mol. Cell. Biol.* (2007)
781 <https://doi.org/10.1128/mcb.01380-07>.
- 782 44. G. A. Challen, *et al.*, Dnmt3a and Dnmt3b have overlapping and distinct functions
783 in hematopoietic stem cells. *Cell Stem Cell* (2014)
784 <https://doi.org/10.1016/j.stem.2014.06.018>.
- 785 45. W. Zhang, J. Xu, DNA methyltransferases and their roles in tumorigenesis.
786 *Biomark. Res.* (2017) <https://doi.org/10.1186/s40364-017-0081-z>.
- 787 46. K. D. Robertson, DNA methylation, methyltransferases, and cancer. *Oncogene*
788 (2001) <https://doi.org/10.1038/sj.onc.1204341>.
- 789 47. R. E. Husni, *et al.*, DNMT3a expression pattern and its prognostic value in lung
790 adenocarcinoma. *Lung Cancer* **97**, 59–65 (2016).
- 791 48. H. R. Davies, *et al.*, Epigenetic modifiers DNMT3A and BCOR are recurrently
792 mutated in CYLD cutaneous syndrome. *Nat. Commun.* **10**, 1–9 (2019).
- 793 49. J. Zhang, E. Bardot, E. Ezhkova, Epigenetic regulation of skin: Focus on the
794 Polycomb complex. *Cell. Mol. Life Sci.* **69**, 2161–2172 (2012).
- 795 50. K.-M. Noh, *et al.*, Engineering of a Histone-Recognition Domain in Dnmt3a Alters
796 the Epigenetic Landscape and Phenotypic Features of Mouse ESCs. *Mol. Cell*
797 (2018) <https://doi.org/10.1016/j.molcel.2018.01.014>.
- 798 51. D. N. Weinberg, *et al.*, The histone mark H3K36me2 recruits DNMT3A and

- 799 shapes the intergenic DNA methylation landscape. *Nature* **573**, 281–286 (2019).
- 800 52. B. Kuehlmann, C. A. Bonham, I. Zucal, L. Prantl, G. C. Gurtner,
801 Mechanotransduction in Wound Healing and Fibrosis. *J. Clin. Med.* **9**, 1423
802 (2020).
- 803 53. S. Li, D. Yang, L. Gao, Y. Wang, Q. Peng, Epigenetic regulation and
804 mechanobiology. *Biophys. Reports* **6**, 33–48 (2020).
- 805 54. H. Q. Le, *et al.*, Mechanical regulation of transcription controls Polycomb-
806 mediated gene silencing during lineage commitment. *Nat. Cell Biol.* **18**, 864–875
807 (2016).
- 808 55. M. M. Nava, *et al.*, Heterochromatin-Driven Nuclear Softening Protects the
809 Genome against Mechanical Stress-Induced Damage. *Cell* (2020)
810 <https://doi.org/10.1016/j.cell.2020.03.052>.
- 811 56. Y. Ling, *et al.*, Modification of de novo DNA methyltransferase 3a (Dnmt3a) by
812 SUMO-1 modulates its interaction with histone deacetylases (HDACs) and its
813 capacity to repress transcription. *Nucleic Acids Res.* **32**, 598–610 (2004).
- 814 57. B. Li, *et al.*, Polycomb protein Cbx4 promotes SUMO modification of de novo DNA
815 methyltransferase Dnmt3a. *Biochem. J.* **405**, 369–378 (2007).
- 816 58. E. Rognoni, G. Walko, The Roles of YAP/TAZ and the Hippo Pathway in Healthy
817 and Diseased Skin. *Cells* **8**, 411 (2019).
- 818 59. F. Li, C. A. Adase, L. J. Zhang, Isolation and culture of primary mouse
819 keratinocytes from neonatal and adult mouse skin. *J. Vis. Exp.* **2017**, 56027
820 (2017).
- 821 60. J. A. Nowak, E. Fuchs, Isolation and culture of epithelial stem cells. *Methods Mol.*
822 *Biol.* (2009) https://doi.org/10.1007/978-1-59745-060-7_14.
- 823 61. D. D. Bikle, Z. Xie, C.-L. Tu, Calcium regulation of keratinocyte differentiation.
824 *Expert Rev. Endocrinol. Metab.* **7**, 461–472 (2012).
- 825 62. J. Wu, J. Q. Feng, X. Wang, “In situ hybridization on mouse paraffin sections
826 using DIG-labeled RNA probes” in *Methods in Molecular Biology*, (Humana Press
827 Inc., 2019), pp. 163–171.
- 828 63. J. R. Tse, A. J. Engler, Preparation of hydrogel substrates with tunable
829 mechanical properties. *Curr. Protoc. Cell Biol.* (2010)

- 830 <https://doi.org/10.1002/0471143030.cb1016s47>.
- 831 64. S. Syed, A. Karadaghy, S. Zustiak, Simple polyacrylamide-based multiwell
832 stiffness assay for the study of stiffness-dependent cell responses. *J. Vis. Exp.*
833 **2015** (2015).
- 834 65. M. Brand, S. Rampalli, C. P. Chaturvedi, F. J. Dilworth, Analysis of epigenetic
835 modifications of chromatin at specific gene loci by native chromatin
836 immunoprecipitation of nucleosomes isolated using hydroxyapatite
837 chromatography. *Nat. Protoc.* (2008) <https://doi.org/10.1038/nprot.2008.8>.
- 838 66. S. A. Miller, D. D. Dykes, H. F. Polesky, A simple salting out procedure for
839 extracting DNA from human nucleated cells. *Nucleic Acids Res.* **16**, 1215 (1988).
- 840 67. A. M. Bolger, M. Lohse, B. Usadel, Trimmomatic: A flexible trimmer for Illumina
841 sequence data. *Bioinformatics* **30**, 2114–2120 (2014).
- 842 68. D. Kim, B. Langmead, S. L. Salzberg, HISAT: A fast spliced aligner with low
843 memory requirements. *Nat. Methods* **12**, 357–360 (2015).
- 844 69. P. D. Thomas, *et al.*, PANTHER: A library of protein families and subfamilies
845 indexed by function. *Genome Res.* (2003) <https://doi.org/10.1101/gr.772403>.
- 846